Evolution of Photon Sources

Caterina Biscari

ALBA Synchrotron

Crab Nebula(www.en.wikipedia.org/wiki/Pulsar)

Electromagnetic radiation

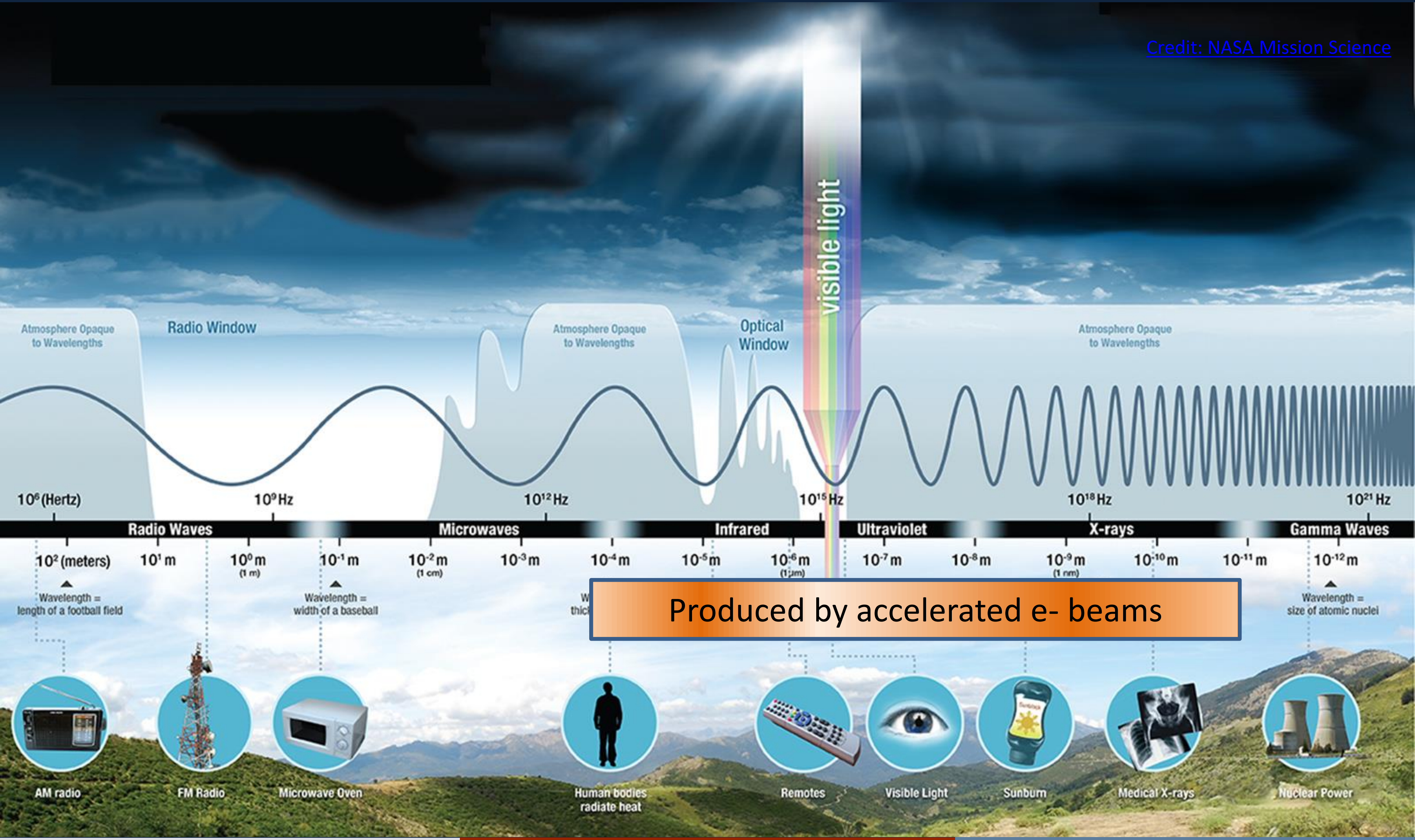

Produced by accelerated e- beams

The first synchrotron light

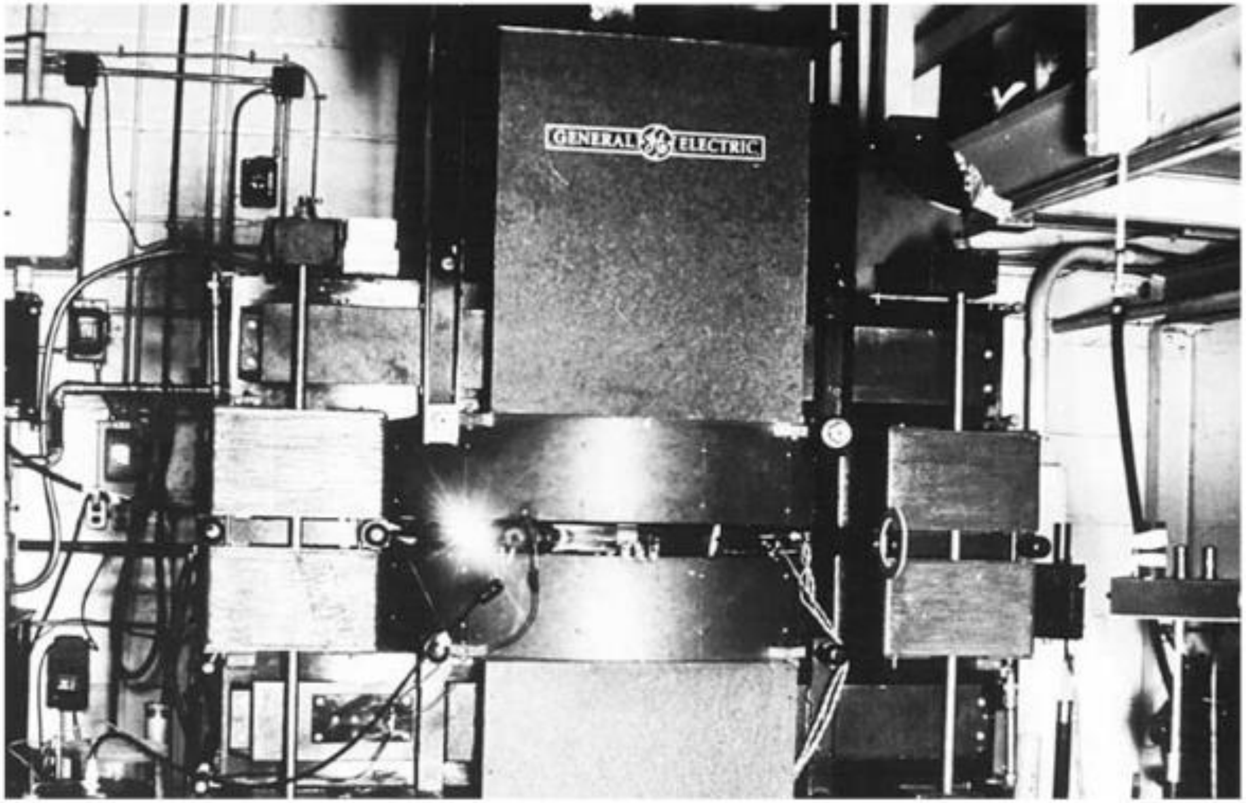

This 300 MeV electron synchroton at the General Electric Co. at Schenectady, built in the late 1940s. The photograph shows a beam of synchrotron radiation emerging.

E.Wilson, Accelerator theory, 7-12-2011

Producing the synchrotron light

electrons accelerated to almost velocity of light and introduced in a magnetic field are bent and emit photons

covering a wide range of wavelengths

depending on e- energy + magnetic field strength

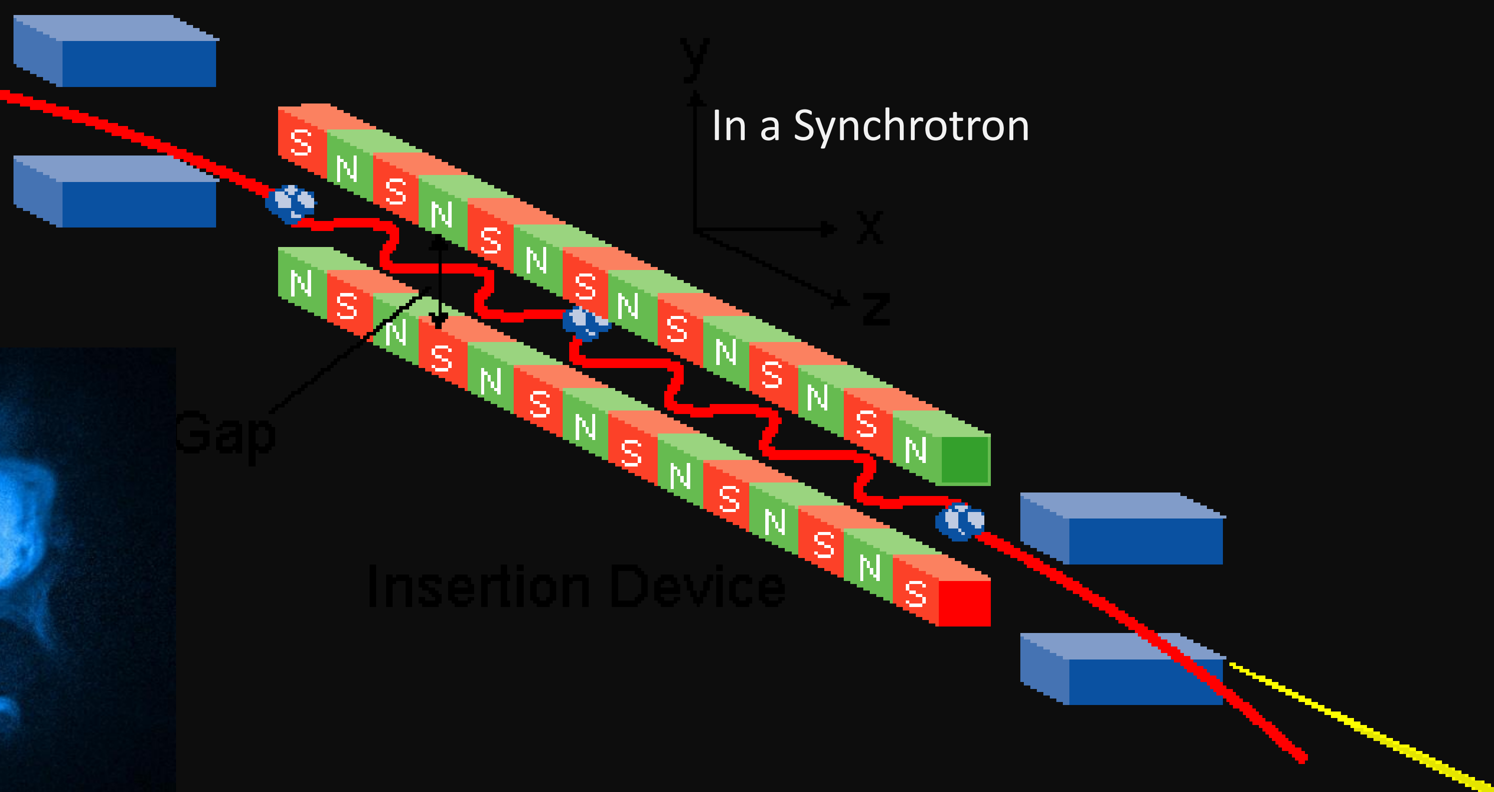

Interaction of light with matter

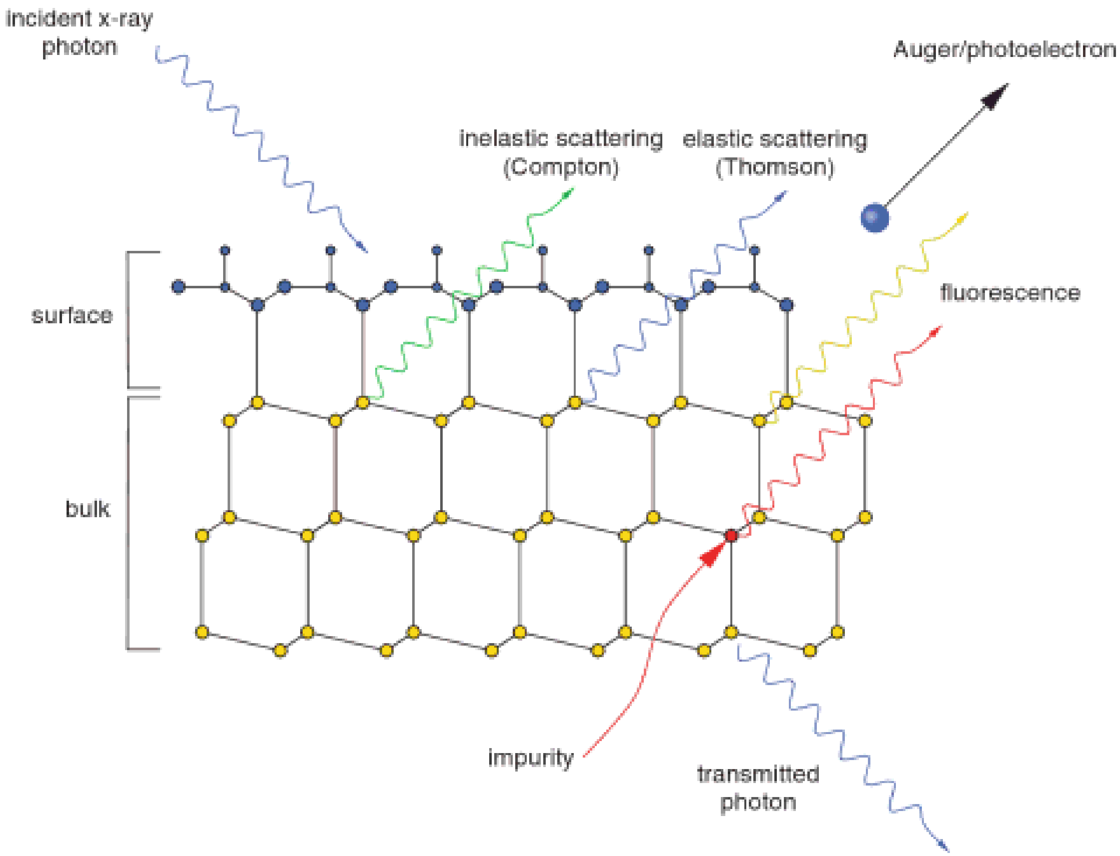

Figure 2.1 *The interaction of x-rays with matter. Surface (and interface) regions of a solid or liquid material are characterized by physical properties and structures that may differ significantly from those of the bulk structure. The x-rays may be elastically or inelastically scattered, or absorbed, in which case electrons or lower-energy photons can be emitted. If none of the above occur, the photon is transmitted through the sample.*

From 'An Introduction to Synchrotron Radiation' Philip Willmott

Photons and electrons produced by the interaction carry information on matter structure and composition

"The usefulness of synchrotron light is limited only by our imagination"
Sir Gustav Nossal

Brightness

Photon flux [photons/s/0.1% bw]

$$B(\lambda) \propto \frac{F(\lambda)}{\left(\epsilon_{x,e^-} \otimes \epsilon_r(\lambda)\right)\ \left(\epsilon_{y,e^-} \otimes \epsilon_r(\lambda)\right)}$$

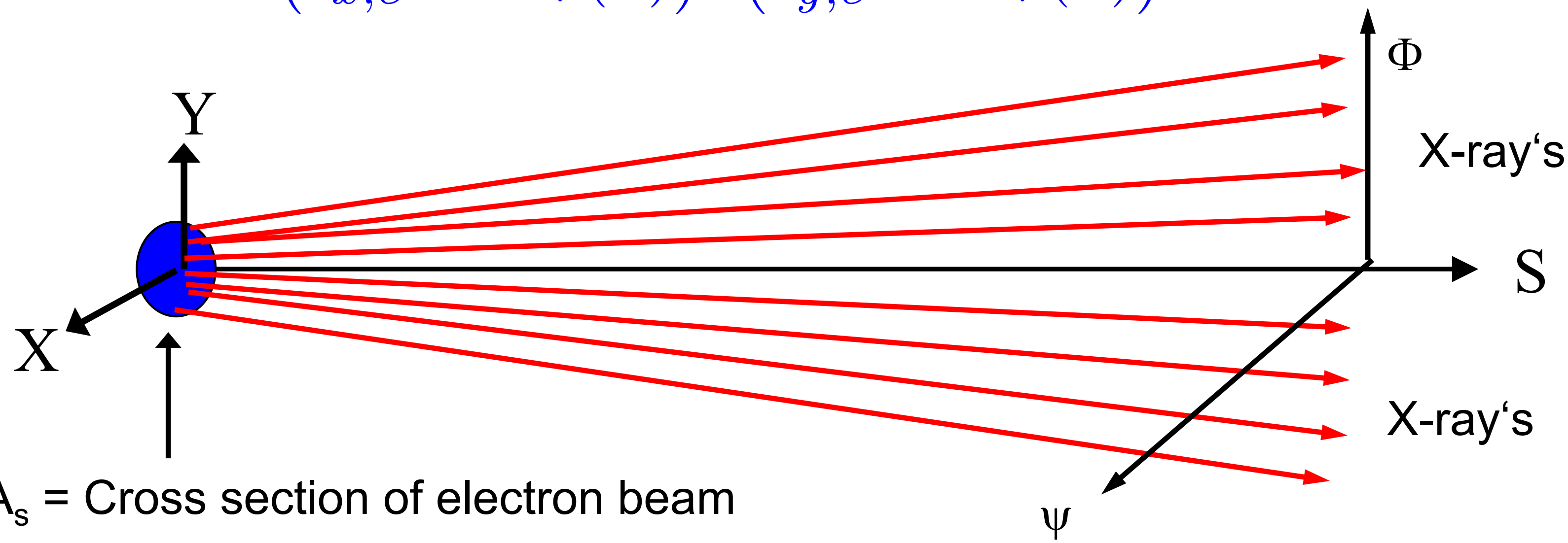

A_s = Cross section of electron beam

Emittance (size and divergence)

The brilliance represents the number of photons per second emitted in a given bandwidth that can be refocus by a perfect optics on the unit area at the sample.

Storage ring spectral brilliance (brightness)

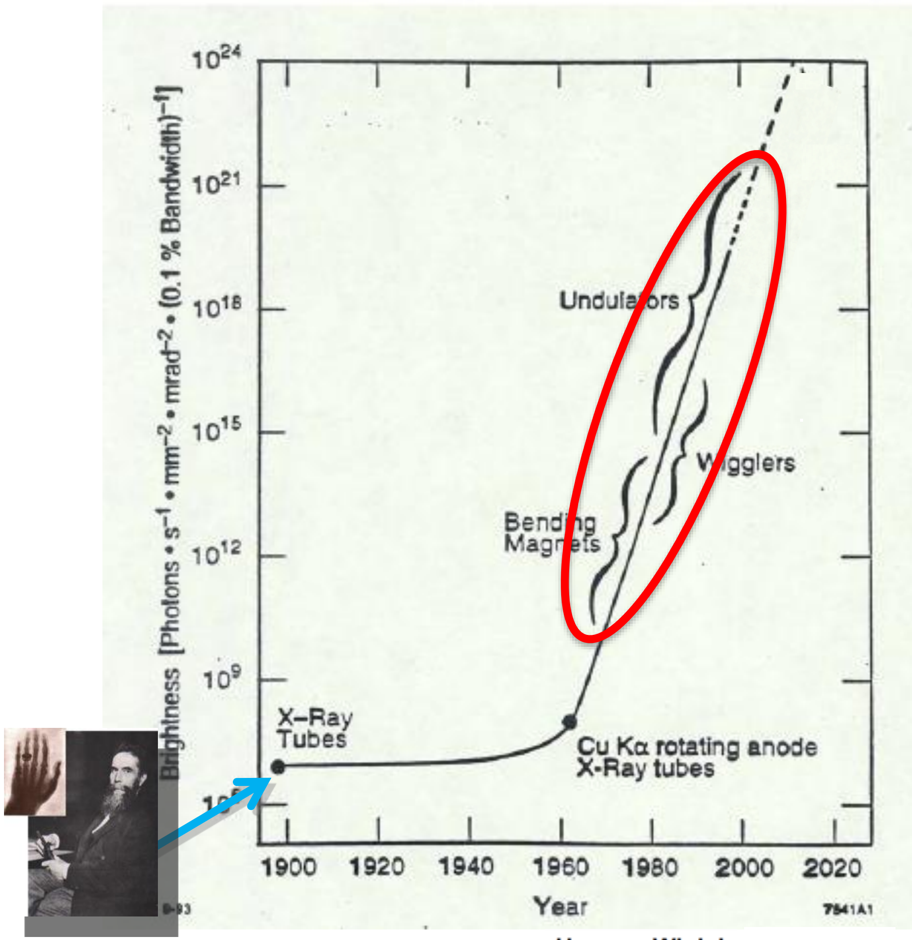

Herman Winick March 26, 2007

4th Generation

emittance reduction with MBA lattices, high performance IDs, high coherent flux

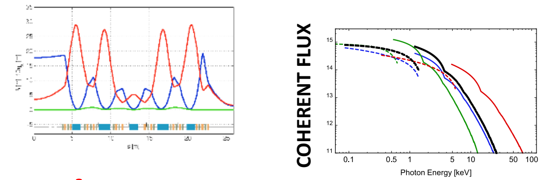

3rd Generation

DBA, TBA lattices with straight sections for wigglers and undulators, high brilliance

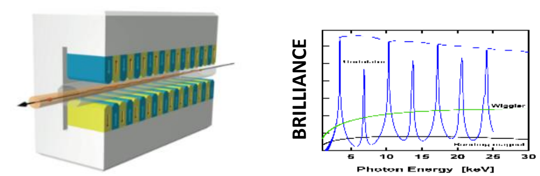

2nd Generation

dedicated sources from bending magnets, high flux

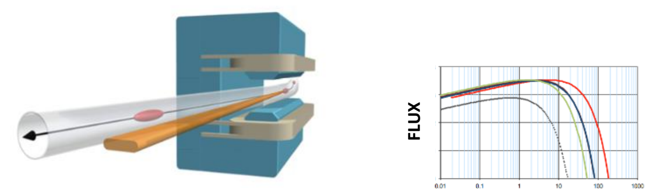

1st Generation

parasitic operation in colliders, bending magnets

From Liu Lin, LNLS, IPAC17

The latest generations of storage rings

emittance scaling $\epsilon_0 \propto \dfrac{\gamma^2}{N_B^3}$

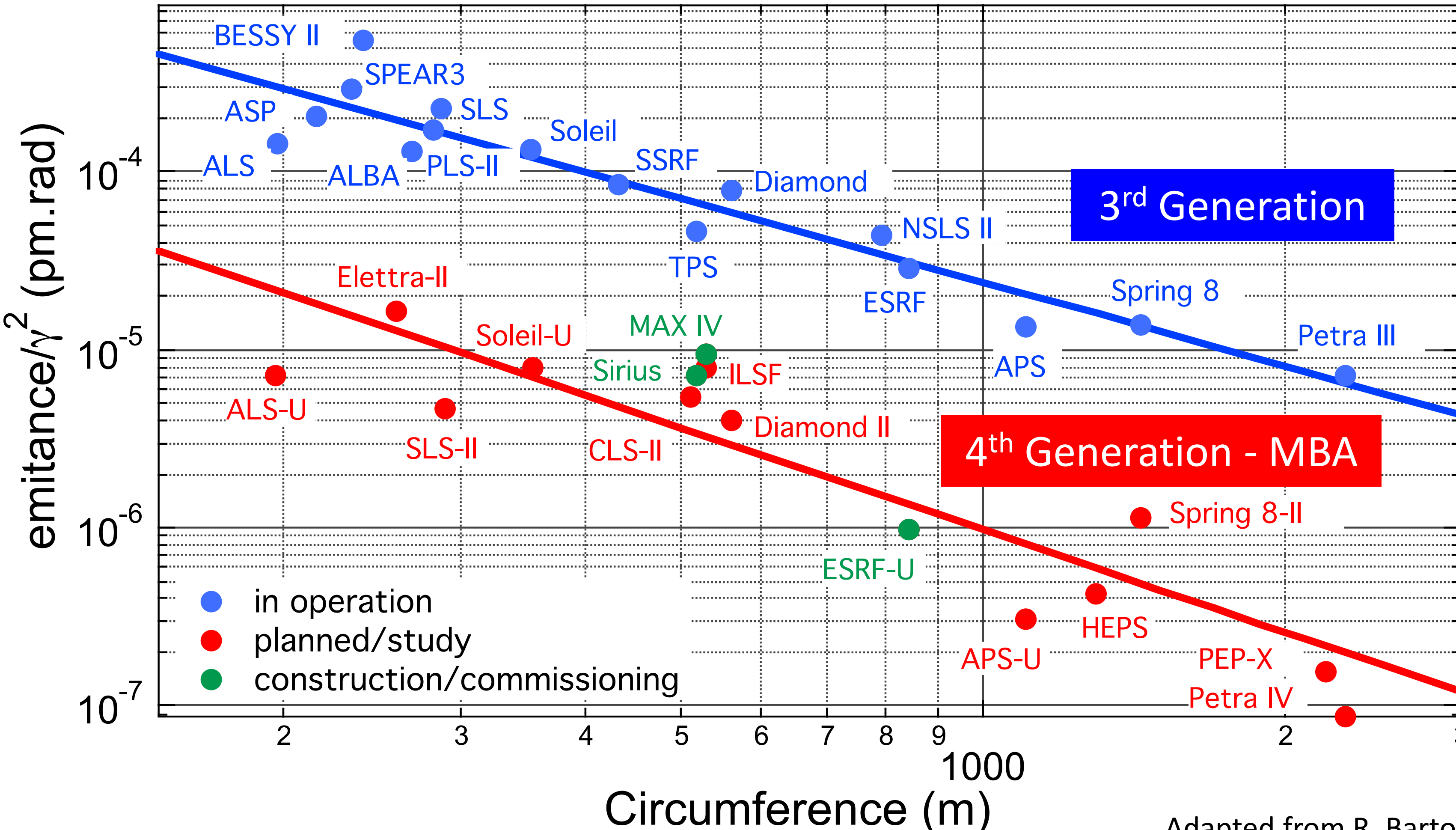

Adapted from R. Bartolini

Achieving low emittance with MBA

Emittance depends on optics at places where radiation is emitted (dipoles).

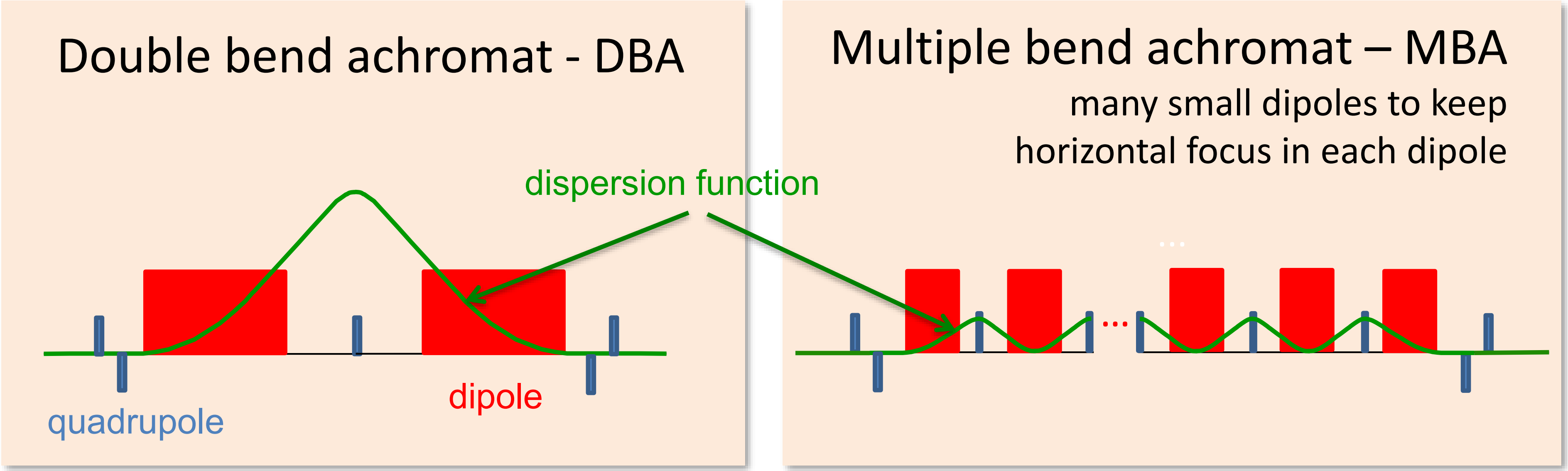

From Liu Lin, LNLS, IPAC17

From 3rd generation of beginning of century to USR

ALBA
2011 1st beam
3 GeV
C = 269 m
ε = 4.6 nm

Increase C x 3
Lower ε x 3

NSLS II
2014 1st beam
3 GeV
C = 792 m
ε = 1.5 nm

MAX IV
2015 1st beam
3 GeV
C = 528 m
ε = 0.3 nm

MBA*
Increase C x 2
Lower ε x 10

*MBA: Multi Bend Achromats

(Photos approximately in scale)

The evolution of light source technologies in a single lab

MAX IV

3.0 GeV

1.5 GeV

2017

ε = 300pm

MAX IV
3.0 GeV
1.5 GeV
2017
ε = 300pm

The evolution to DLSR or USR (Diffraction Limited or Ultimate Storage Rings)

Even in the limit of zero beam emittance the phase space of the radiation emission from an undulator is itself finite due to diffraction effects at the source. For single-mode photon emission, the corresponding diffraction-limited 'emittance' of the photon beam is given by

$$\varepsilon(photon) \leq \frac{\lambda}{4\pi} = 0.159\lambda = 98.66[pm\, rad]/E_{\gamma}[keV]$$

A light source is referred as 'diffraction limited' when the e beam emittance is less than that of the radiated photon beam at the desired X-ray wavelength

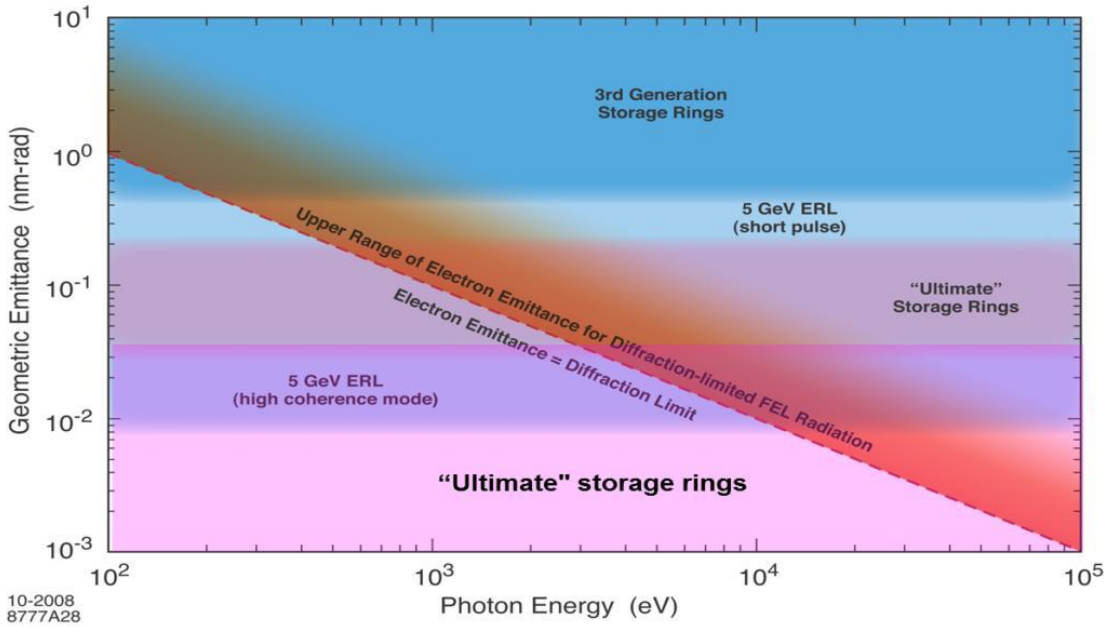

Storage rings going brighter by Making very low emittances:

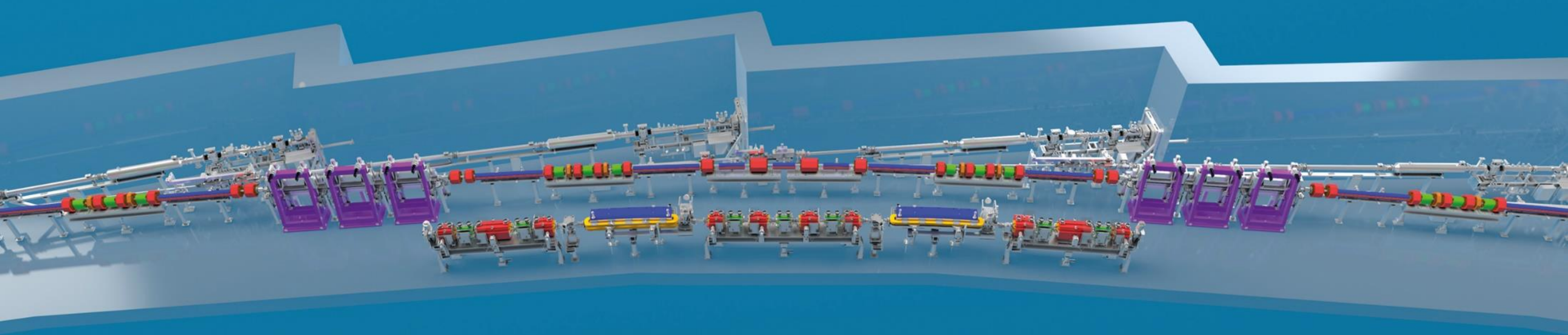

ESRF: brighter beams by 2020

Other facilities planning upgrades

Tunability, polarization

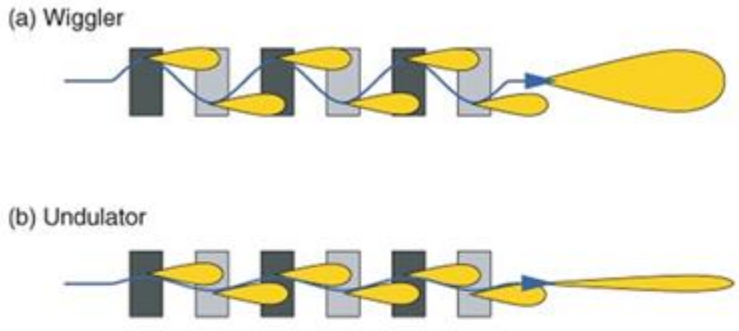

wiggler - incoherent superposition K > 1
Max. angle of trajectory > $1/\gamma$

undulator - coherent interference K < 1
Max. angle of trajectory < $1/\gamma$

$$K = \frac{e}{2\pi m_o c} B_o \lambda_u$$

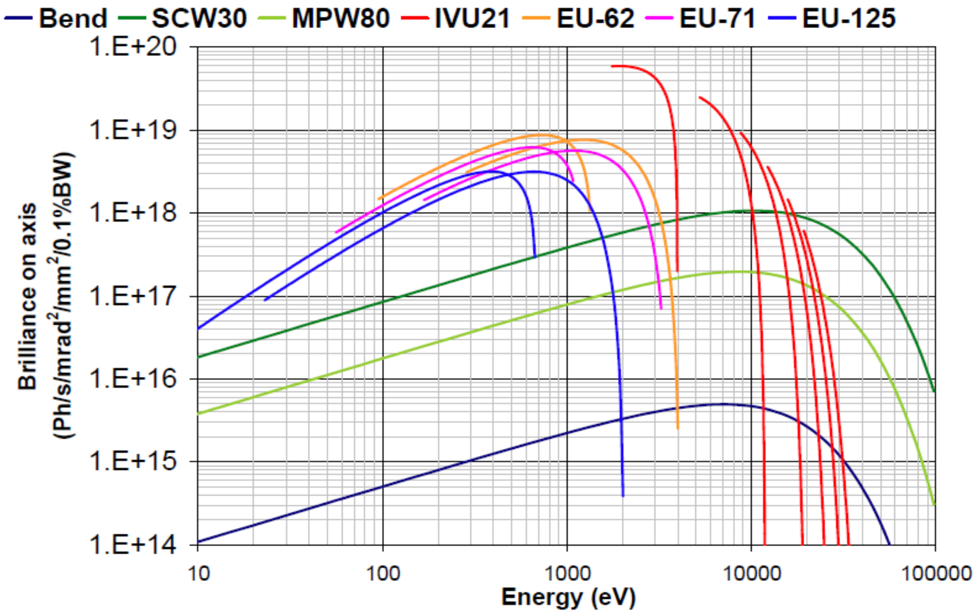

Tuning ID magnetic field and orientation, and playing with beamline optical elements large range of photon energy and polarization are available

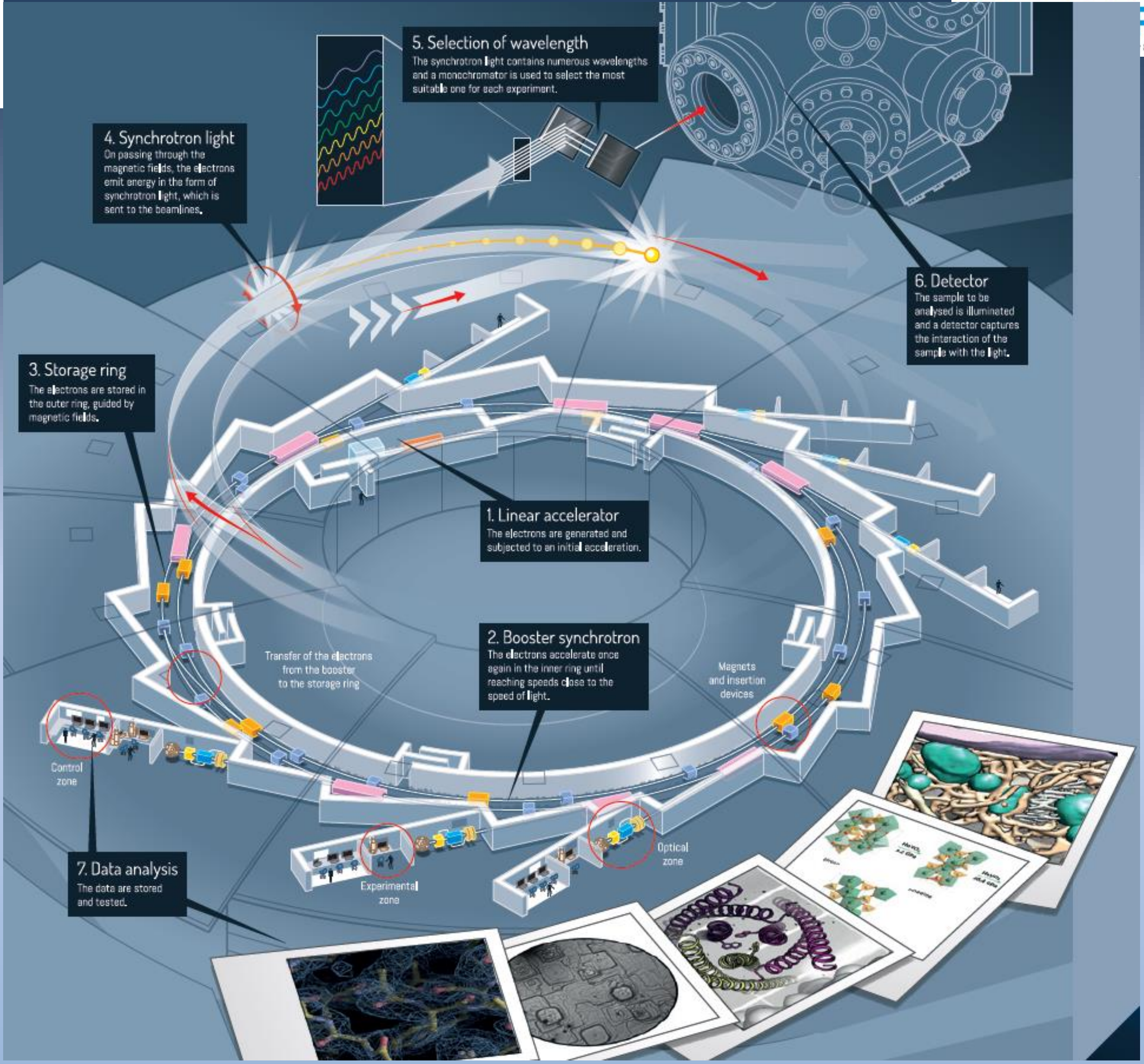

5. Selection of wavelength
The synchrotron light contains numerous wavelengths and a monochromator is used to select the most suitable one for each experiment.
4. Synchrotron light
On passing through the magnetic fields, the electrons emit energy in the form of synchrotron light, which is sent to the beamlines.
6. Detector
The sample to be analysed is illuminated and a detector captures the interaction of the sample with the light.
3. Storage ring
The electrons are stored in the outer ring, guided by magnetic fields.
1. Linear accelerator
The electrons are generated and subjected to an initial acceleration.
2. Booster synchrotron
The electrons accelerate once again in the inner ring until reaching speeds close to the speed of light.
Transfer of the electrons from the booster to the storage ring
Magnets and insertion devices
Control zone
Experimental zone
Optical zone
7. Data analysis
The data are stored and tested.

Life science, among others…

- Protein characterization
- Imaging of biological structures at cell dimensions
- Single-cell analysis, tissue analysis and bacterial identification
- Study of human and animal tissues and their reaction to drugs
- Drug development
- Food science
- Cosmetics
- Study of effects of nanomedicine in tissues

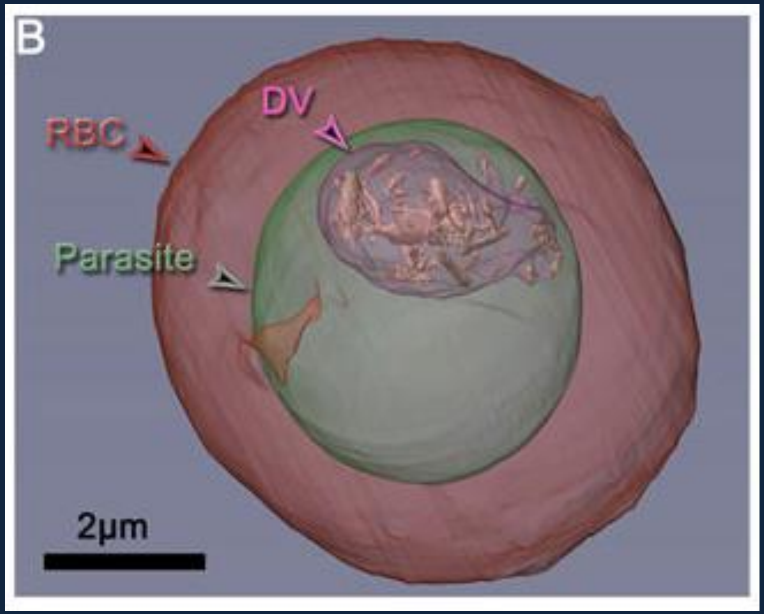

Material science, among others…

- Magnetic properties of material (see figure of skyrmions)
- Development of new catalysts
- Characterization of material for energy transfer and storing
- Soil analysis
- Chemical properties of new materials
- Mineralogical research
- Geochemistry of organic matter and minerals in geological samples
- Analysis of thin films
- Engineering material properties
- Communication technology materials
- Cultural heritage material characterization

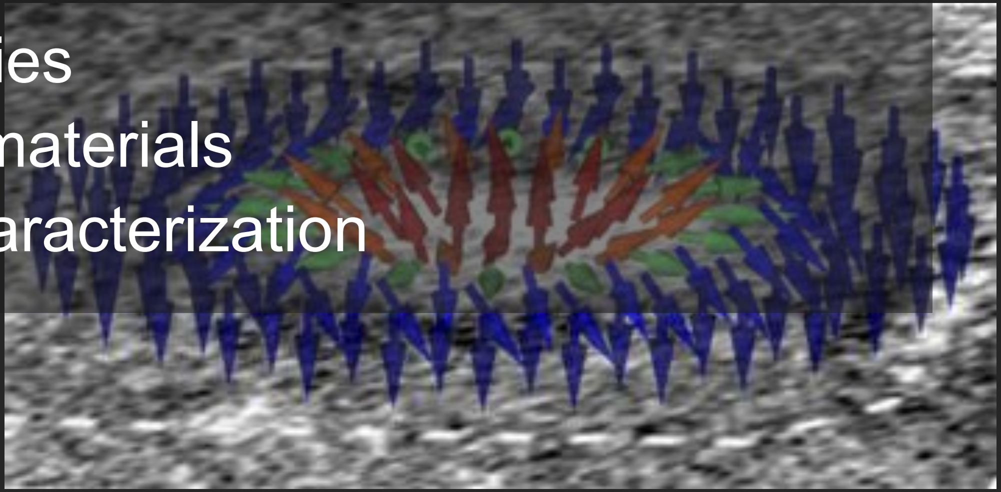

Nobel Prices for research using SL

1997 - Chemistry to Boyer and Walker
2003 - Chemistry to Agre and MacKinnon
2006 – Chemistry to Kornberg
2009 - Chemistry to Ramakrishnan, Steitz and Yonath
2012 - Chemistry to Lefkowitz adnd Kobilka
2013 – Medicine to Rothman, Schekman and Südhof
2013 – Chemistry to Karplus, Levii and Warshel

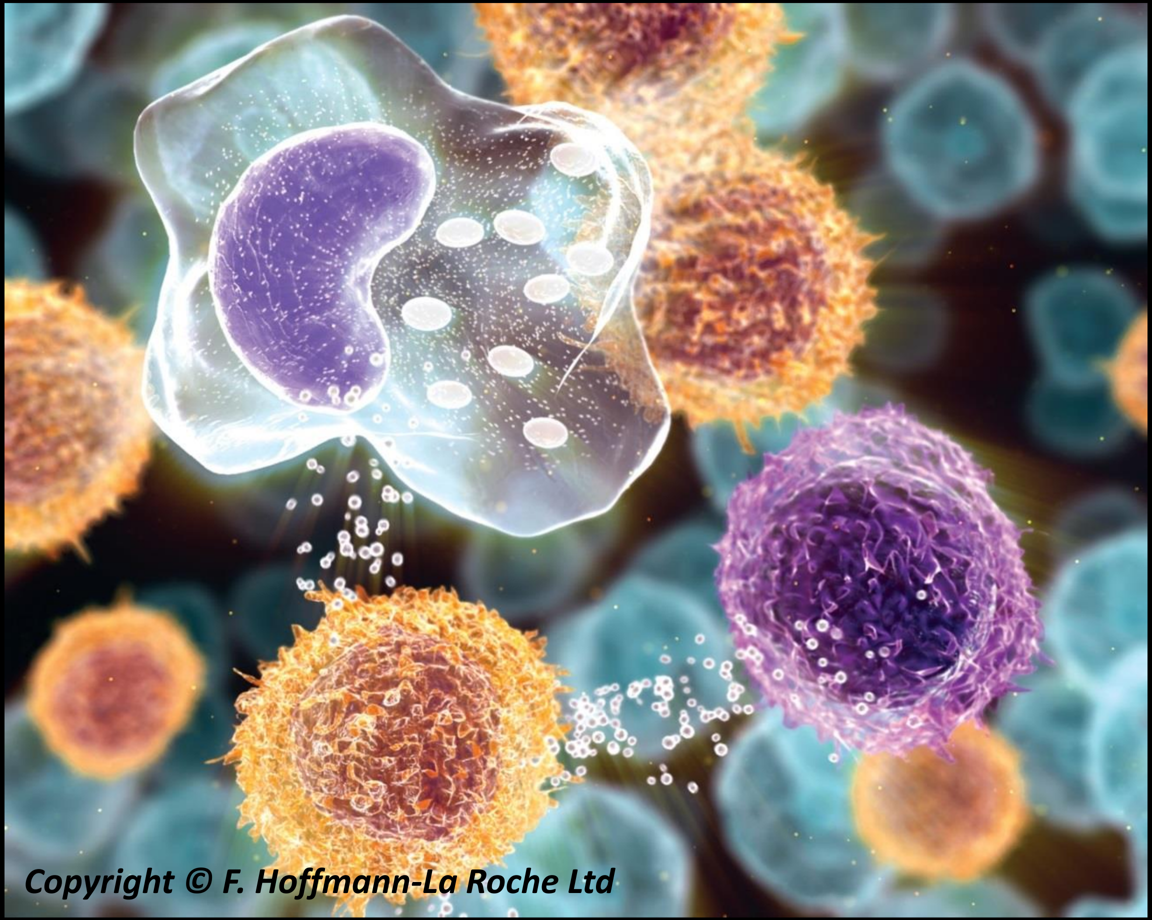

Dr. Peter Doherty, Nobel prize of Medicine: *"Synchrotron light is presently fundamental for 80% of research and development of drugs"*

ALBA Synchrotron

National public institution with 50% national + 50% regional funding (MINECO and GenCat Ministry of Research University and Industry)

National and international (21%) staff

National and international (35%) users

National and international collaborations

Participation to projects plus services providing extra 7-8% of income and 10% of staff

ALBA history

2003
Project approval

2006
Construction start

2012
Operation start
Phase I: 7BLs

2014
Phase II construction start

2016
8th BL in operation
Phase III construction start

2017/2020
Phase III evolution

Design

Construction & commissioning

Operation consolidation

Expansion

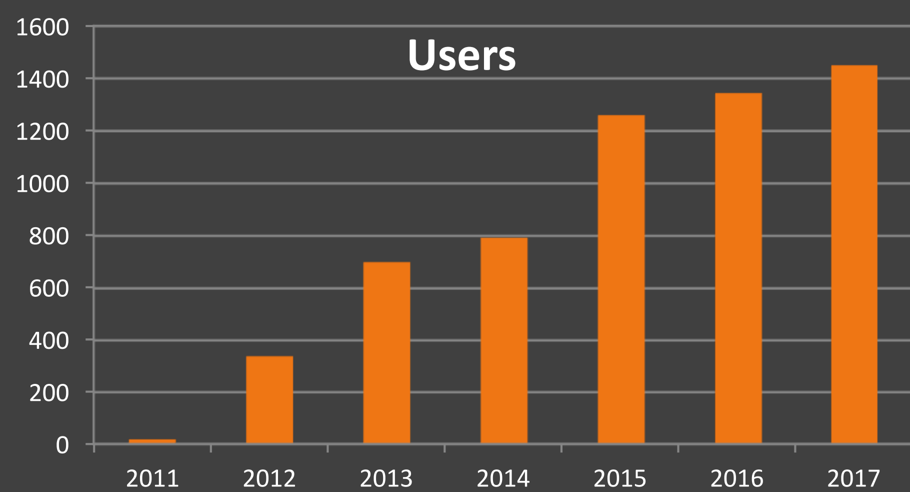

ALBA Accelerators

ALBA : 269 m circumference
3 GeV electrons producing synchrotron light

ALBA beamlines

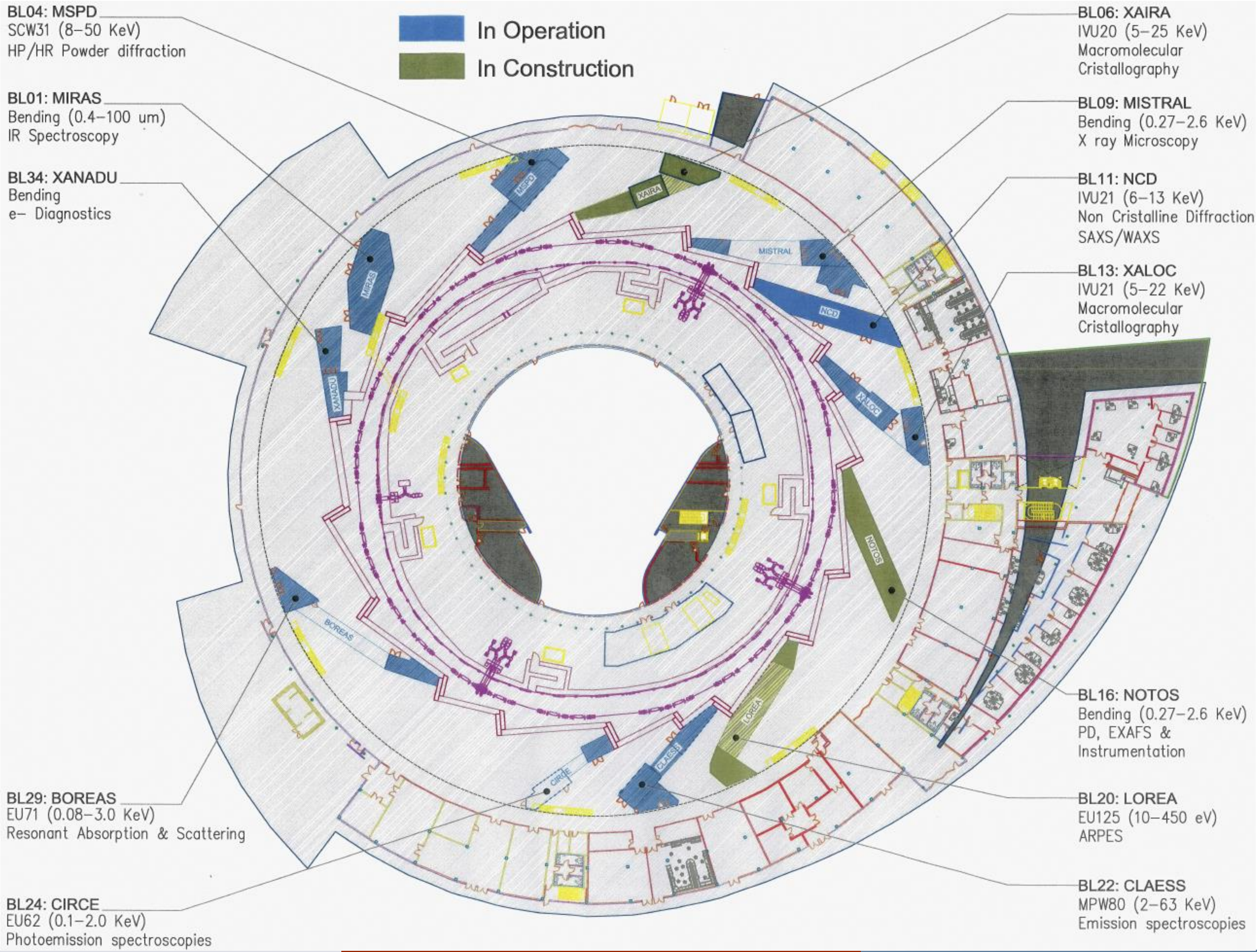

USERS

Competitive and free access
Public results

Academic

Joint academic and industrial

Industrial

Direct access covering operational costs
Private results

ALBA Performance

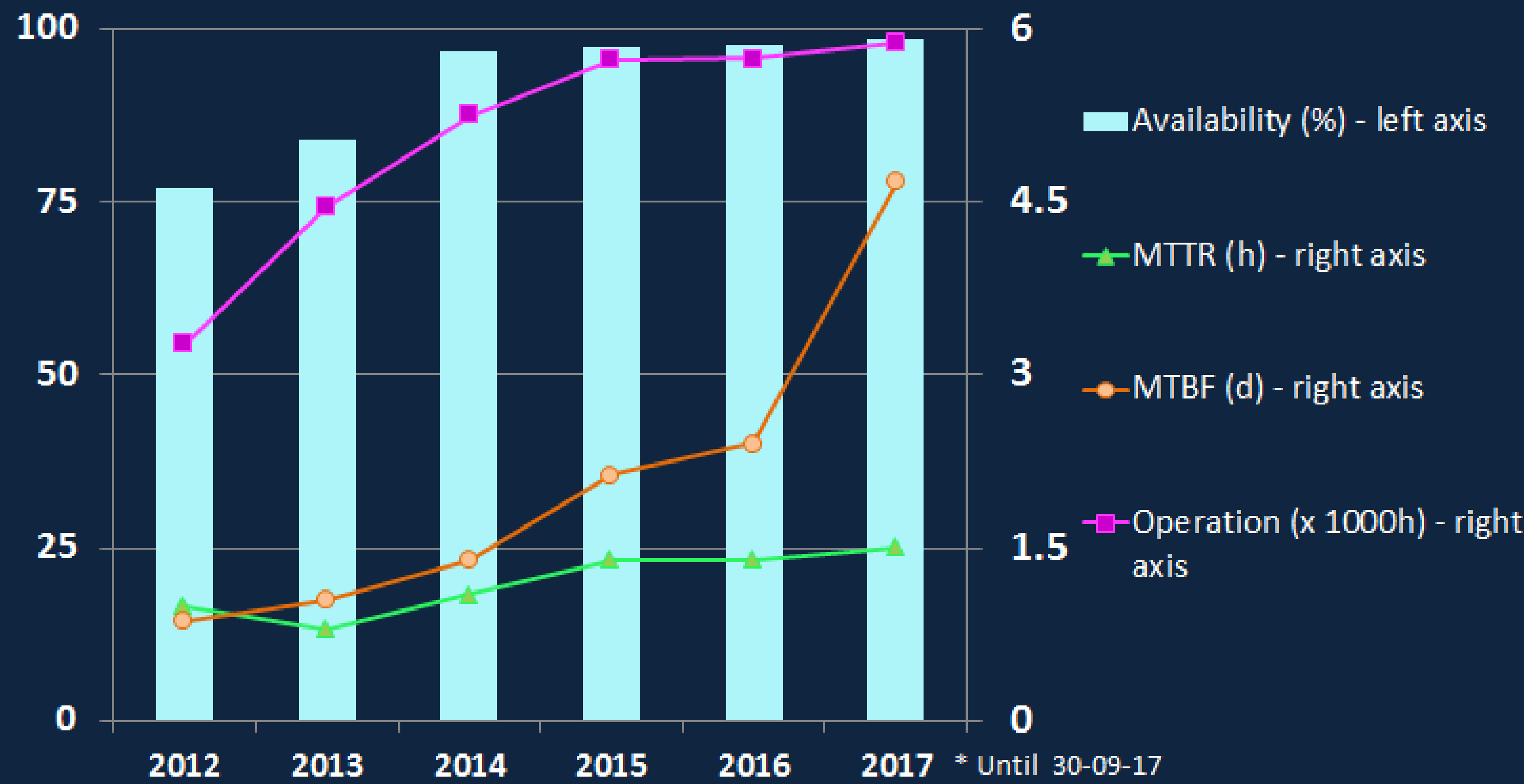

Scientific production

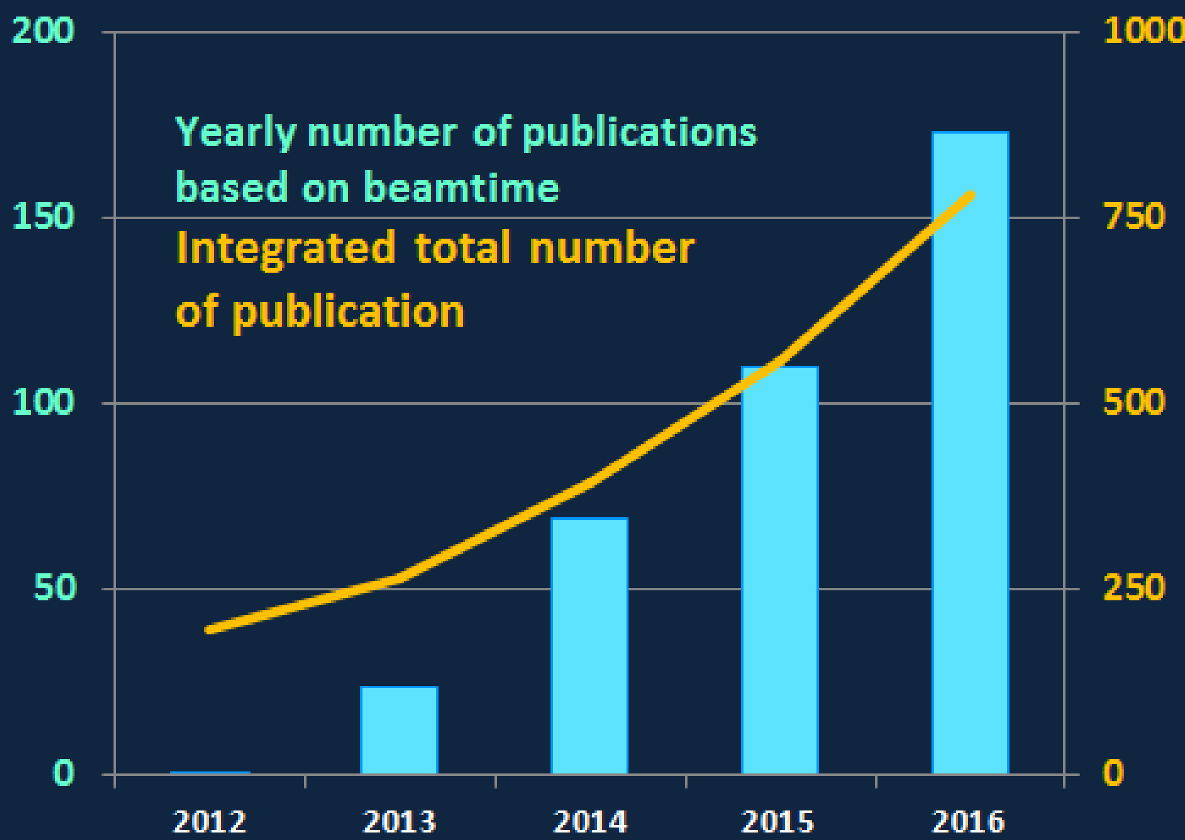

Technology Transfer

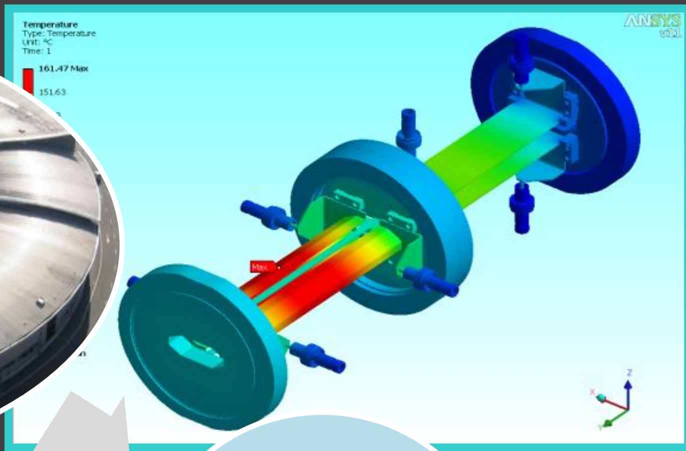

Innovative Designs

Production

Industries

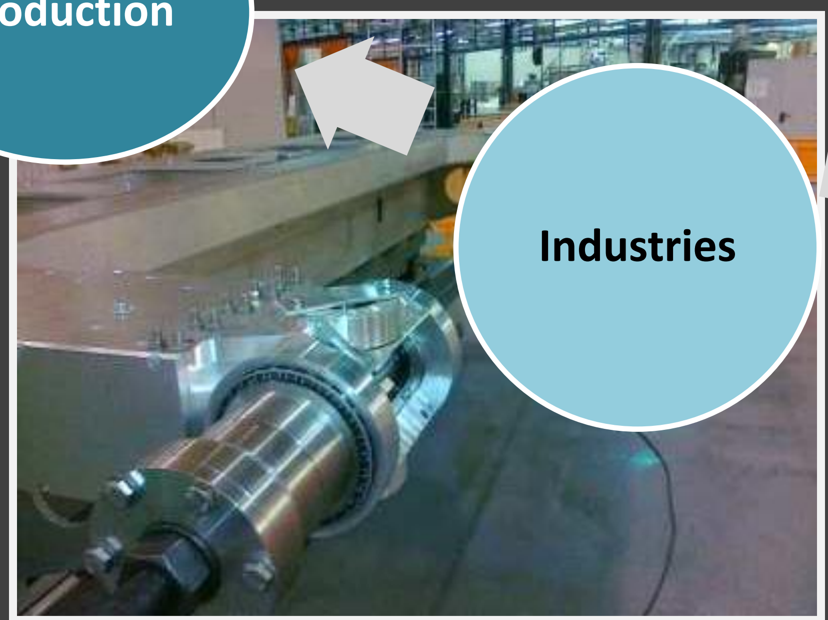

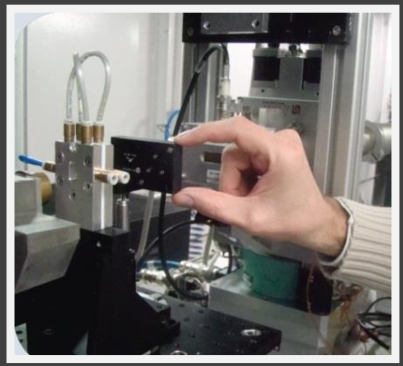

Other scientific infrastructures, national and international

SESAME @ Amman

SESAME Members
Cyprus, Egypt, Iran, Israel, Jordan, Pakistan, Palestinian Authority and Turkey

Location of SESAME

SESAME location in Allan, Jordan

SYNCHROTRON-LIGHT FOR EXPERIMENTAL SCIENCE AND APPLICATIONS IN THE MIDDLE EAST - Developed under the auspices of UNESCO

In commissioning

IPM association

IPM (Institute for Research in Fundamental Sciences of Teheran, under which the ILSF has been created) is associated to ALBA as the first international partner, starting 1st January 2017 with access to 1% of beamtime, to be shared among all beamlines

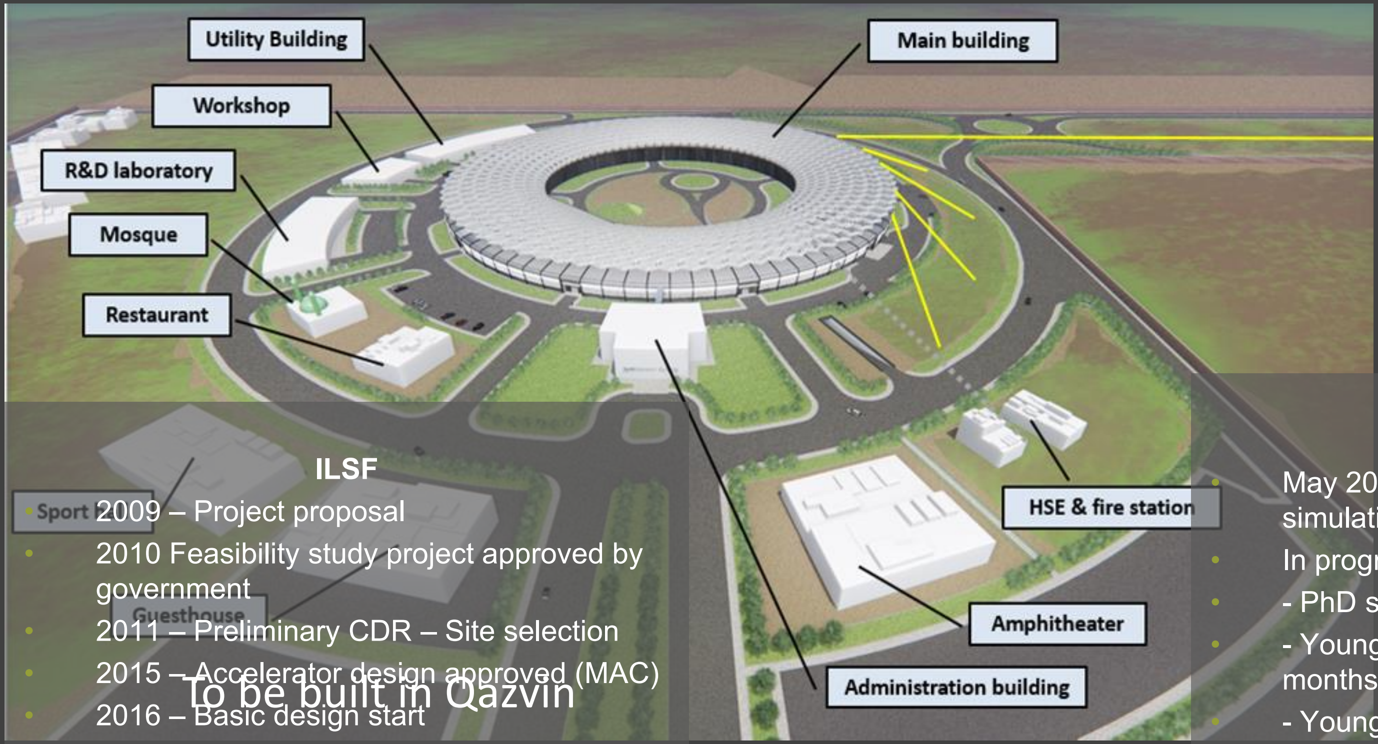

To be built in Qazvin

ILSF

- 2009 – Project proposal
- 2010 Feasibility study project approved by government
- 2011 – Preliminary CDR – Site selection
- 2015 – Accelerator design approved (MAC)
- 2016 – Basic design start
- Technical staff: 48 in 2015, over 90 in 2016
- Developments in RF Power (SSA), magnetic measurements, magnet prototyping, BPM development

Staff training at ALBA

- May 2017 – Student on impedance simulations (5 months)
- In progress for 2017
- - PhD student on BL design
- - Young researcher for beam dynamics (4 months)
- - Young researcher for Controls and Diagnostics (2 weeks)
- - Young researcher on Magnetic Measurements (2 weeks)

IPM association

IPM (Institute for Research in Fundamental Sciences of Teheran, under which the ILSF has been created) is associated to ALBA as the first international partner, starting 1st January 2017 with access to 1% of beamtime, to be shared among all beamlines

First users at ALBA on 26 October 2017

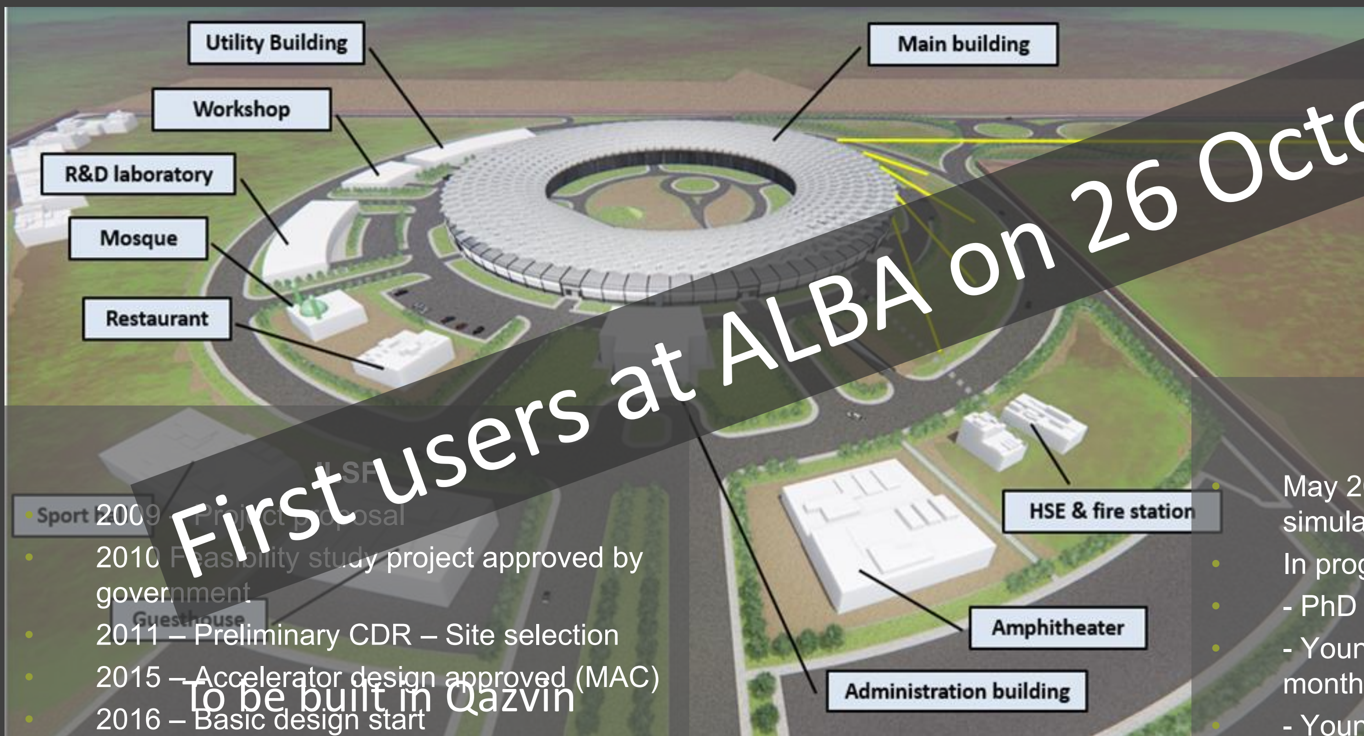

To be built in Qazvin

ILSF

- 2009 – Project proposal
- 2010 Feasibility study project approved by government
- 2011 – Preliminary CDR – Site selection
- 2015 – Accelerator design approved (MAC)
- 2016 – Basic design start
- Technical staff: 48 in 2015, over 90 in 2016
- Developments in RF Power (SSA) , magnetic measurements, magnet prototyping, BPM development

Staff training at ALBA

- May 2017 – Student on impedance simulations (5 months)
- In progress for 2017
- - PhD student on BL design
- - Young researcher for beam dynamics (4 months)
- - Young researcher for Controls and Diagnostics (2 weeks)
- - Young researcher on Magnetic Measurements (2 weeks)

2017: ~ 50 Synchrotrons in the world, serving a community of >50000 users

In Operation *In Commissioning* *In Construction*

LEAPS League of European Accelerator-based Photon Sources

Goals

Secure EU leadership for decades

Develop coherent Roadmap of all SR and FEL facilities in the EU

1) Strong & diverse user community
2) Best practice
3) Push & disseminate technology and innovation
4) Integration & sustainability
5) Enable excellent science
6) Next generation light sources
7) Open science

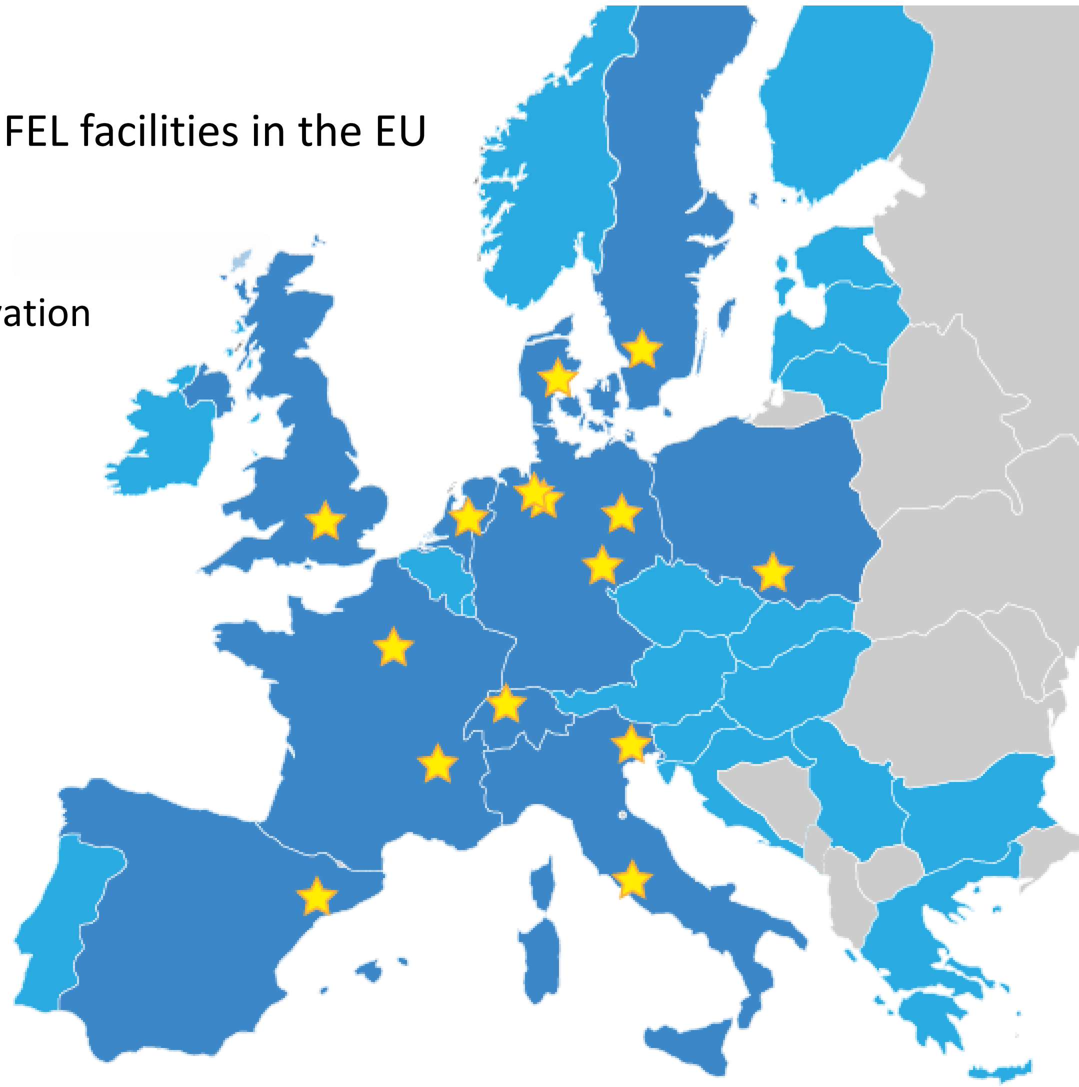

LEAPS Charter

LEAPS Strategy Document (Nov 2017)

Input to EC FP 9 2020-2026

FELS

IN OPERATION   *IN CONSTRUCTION*

FELs are long (km)
Undulators used to produce coherent radiation

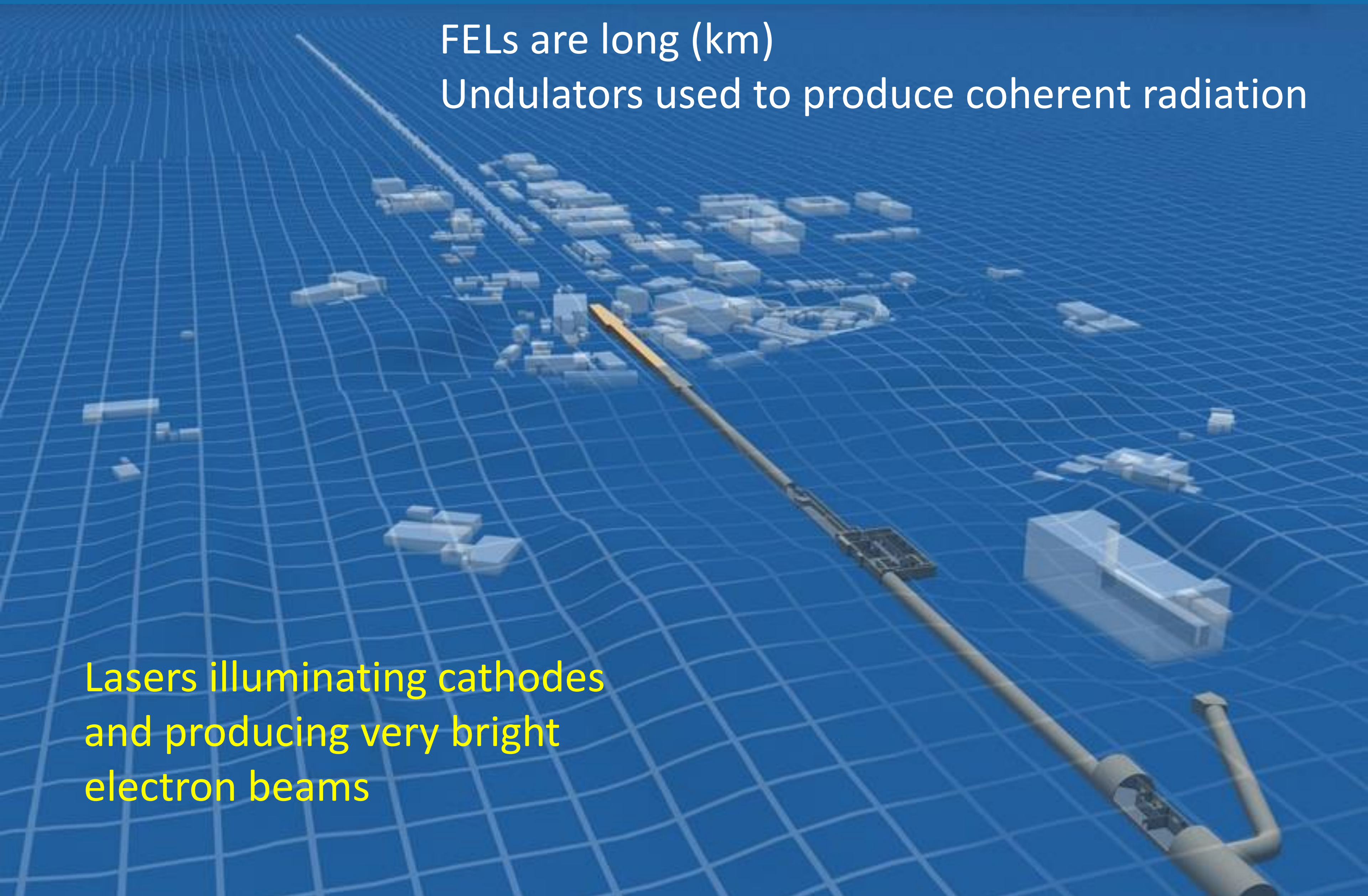

Lasers illuminating cathodes and producing very bright electron beams

Synchrotrons versus FELs

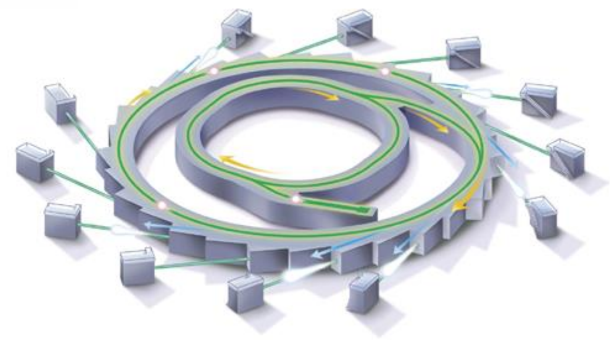

Illustration of the Australian Synchrotron

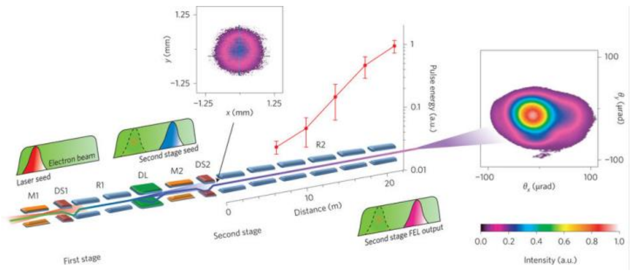

Illustration of FERMI, Nature Photonics 7, 2013

- Multi instrument/user facility (tens of BLs)
- High rep rate
- High stability
- Time structure defined by rf (hundreds of MHz)
- Pulse length in the psec range

- Single instrument/user facility (1/2 BLs)
- Rep rate depending on linac technology
- Time structure defined by rf
- Pulse length in the fsec range
- Brightness increased by coherent emission

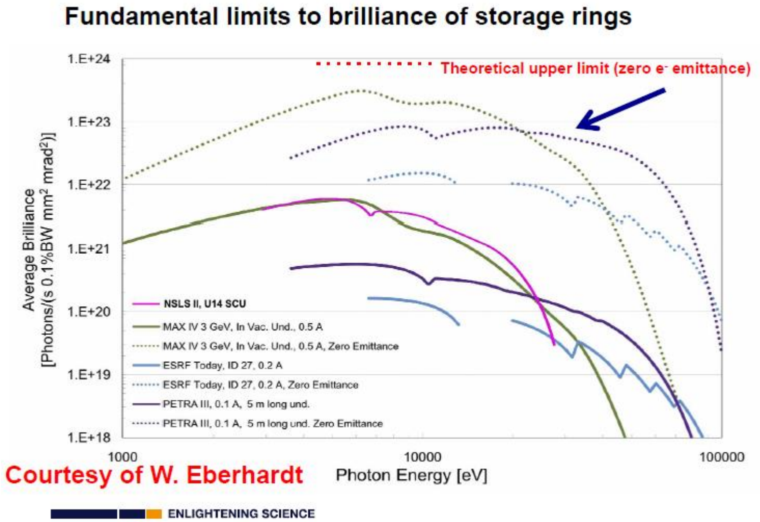

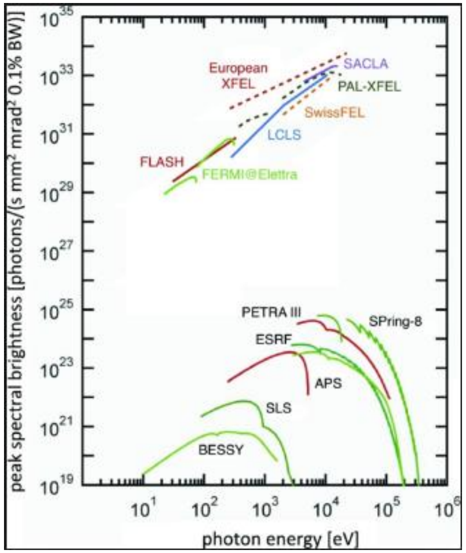

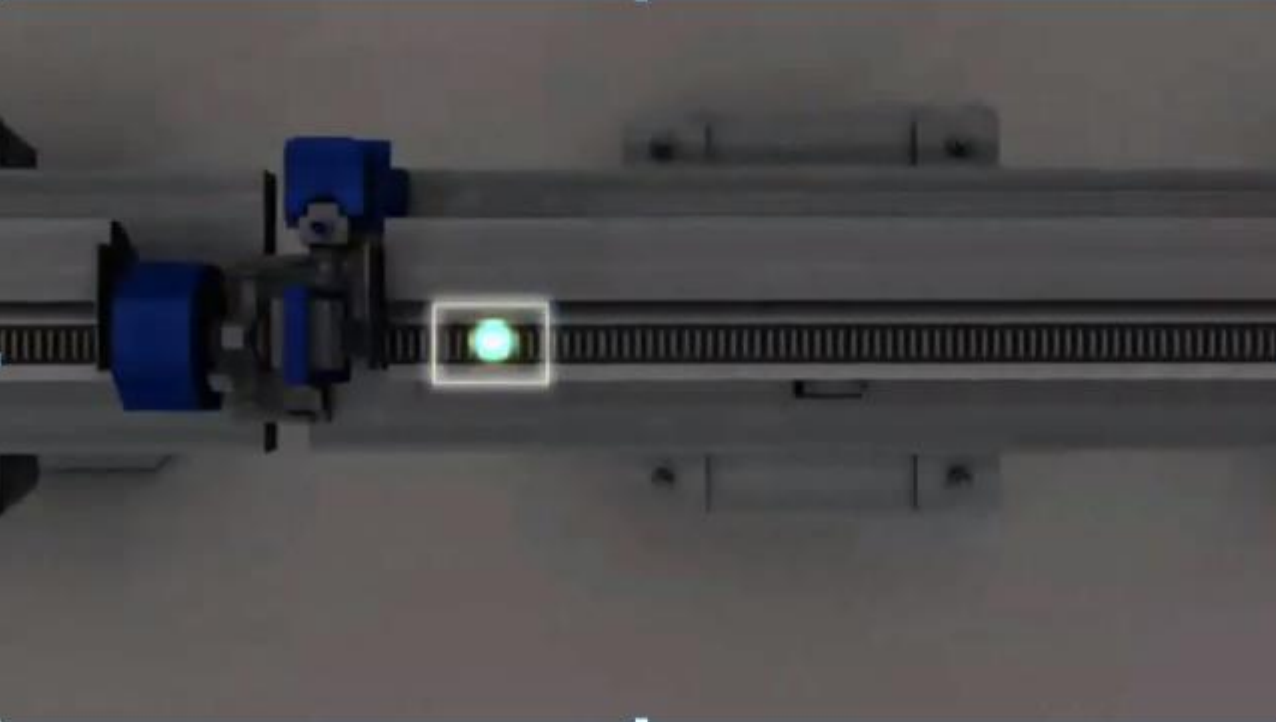

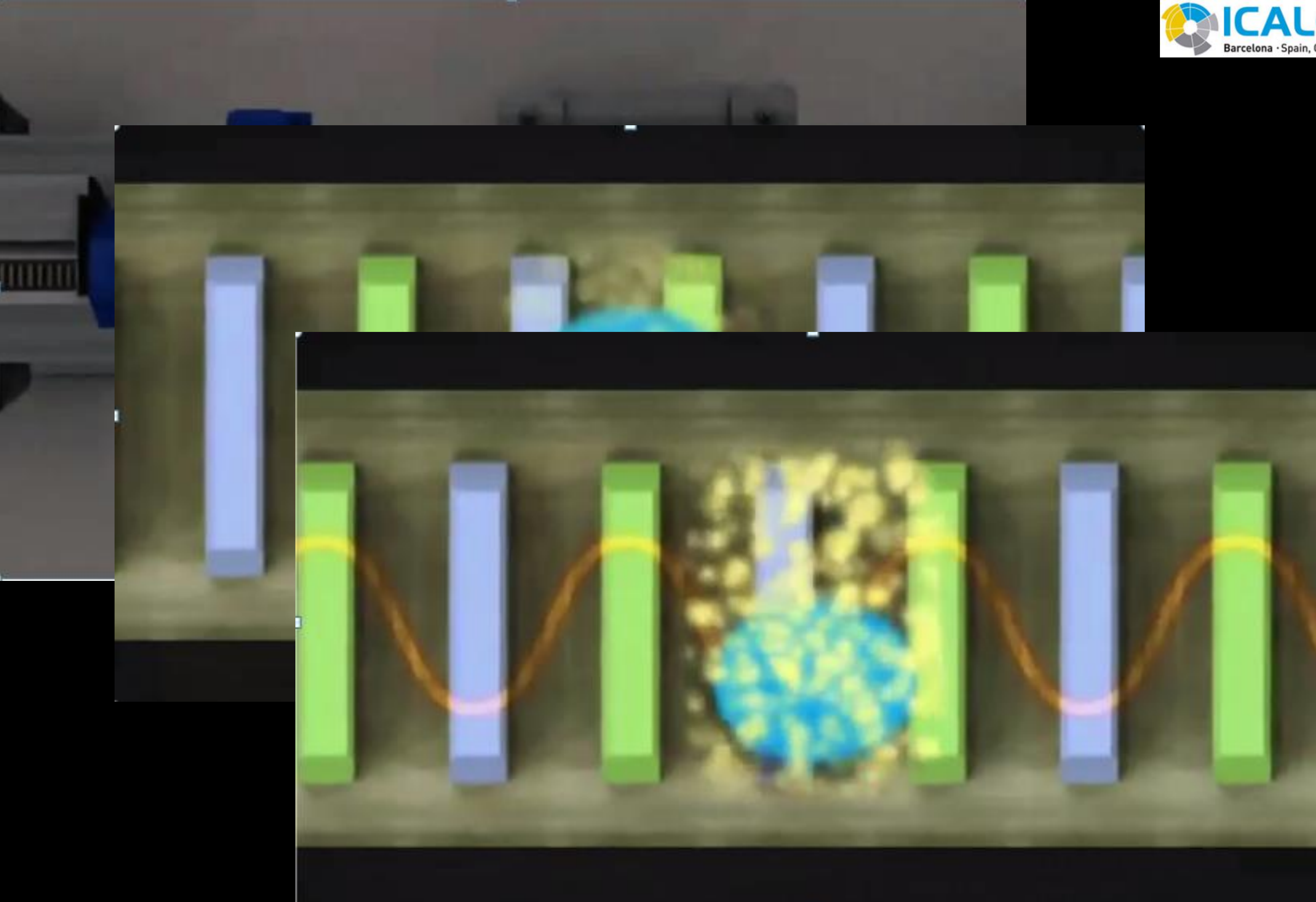

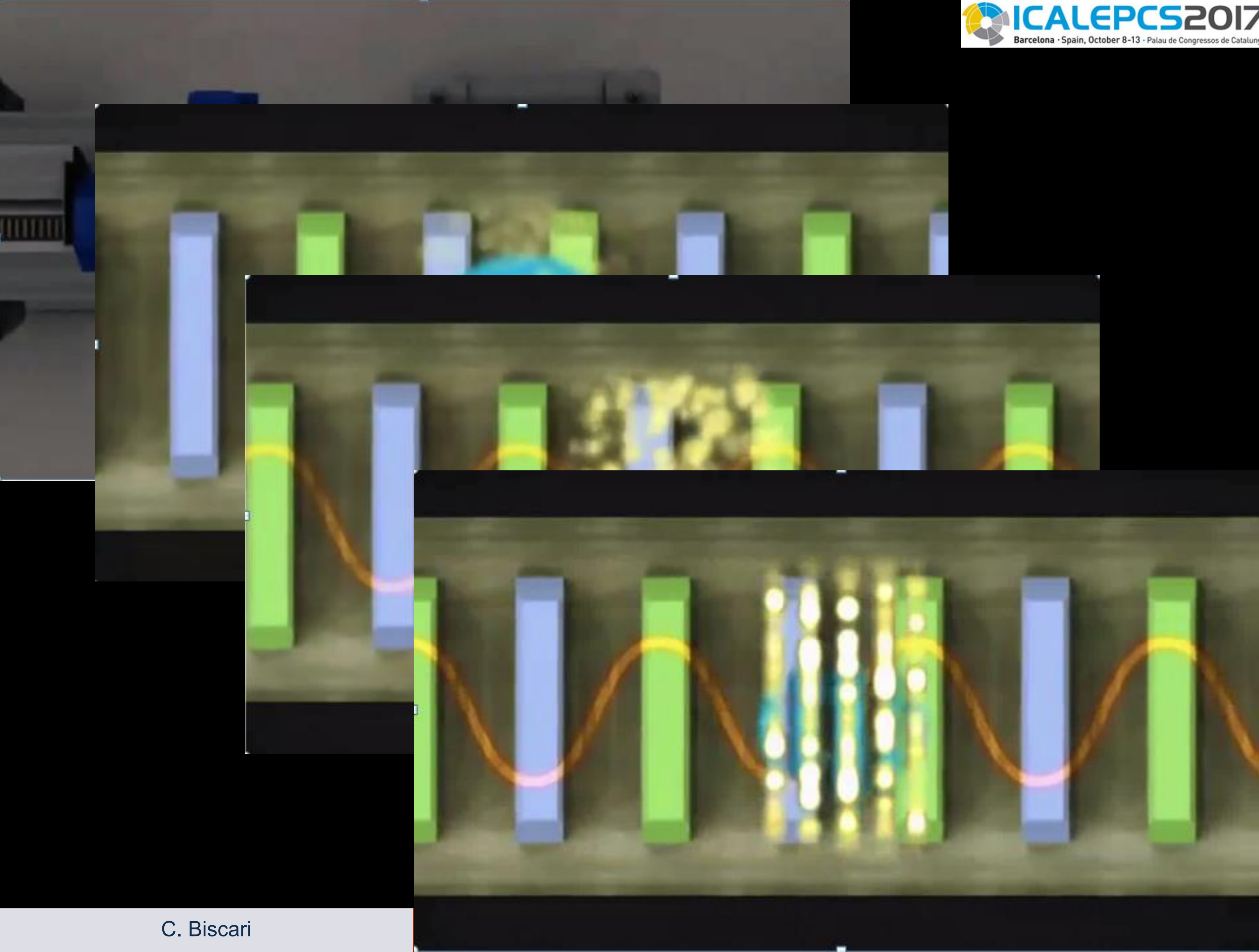

Beating radiation damage: Diffraction before Destruction

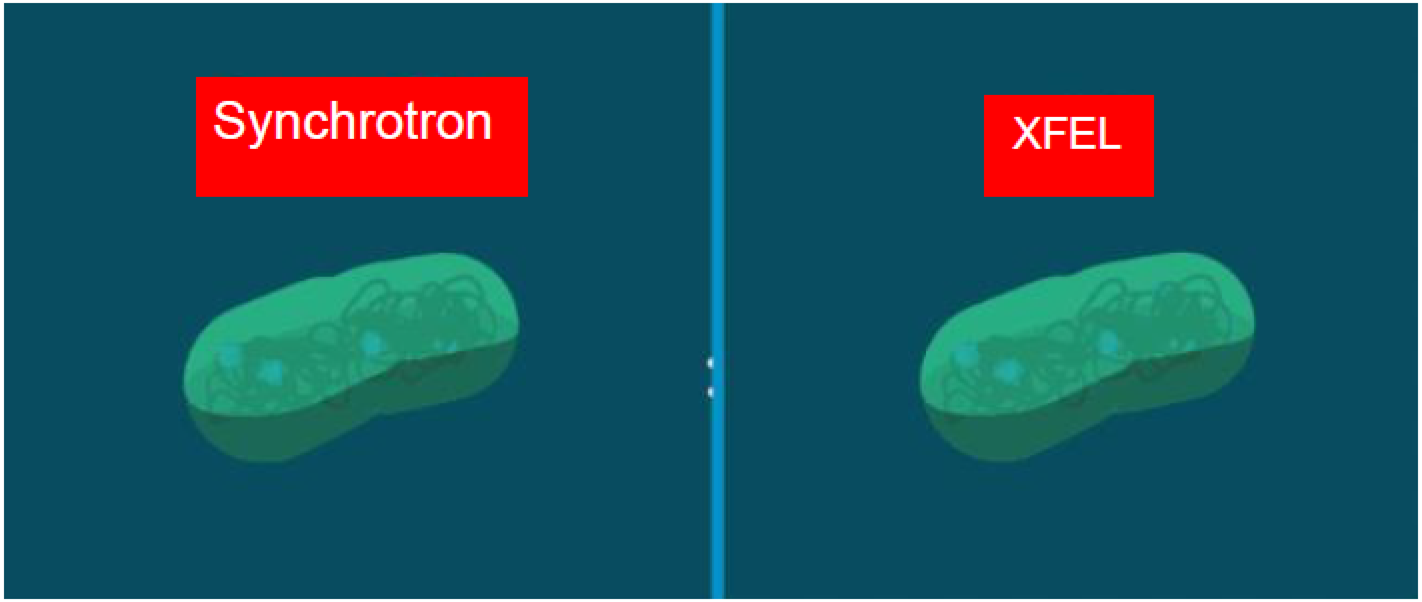

Credits: www.slac.stanford.edu

Beating radiation damage: Diffraction before Destruction

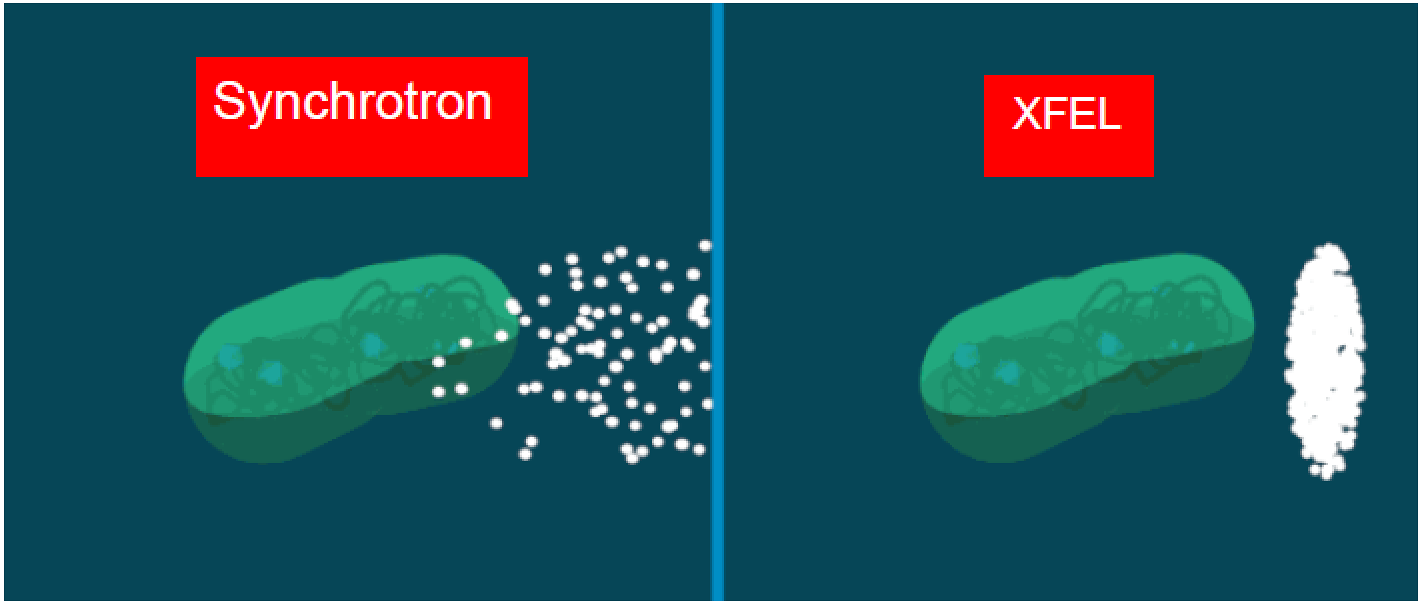

Credits: www.slac.stanford.edu

Beating radiation damage: Diffraction before Destruction

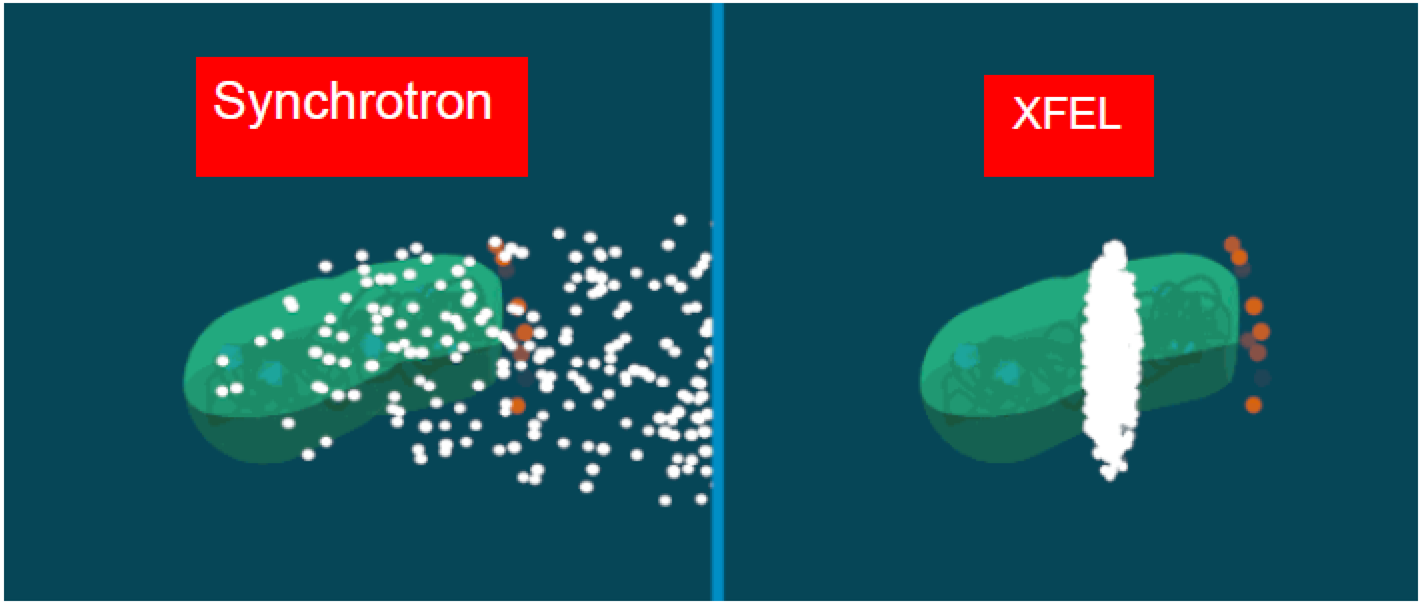

Credits: www.slac.stanford.edu

Beating radiation damage: Diffraction before Destruction

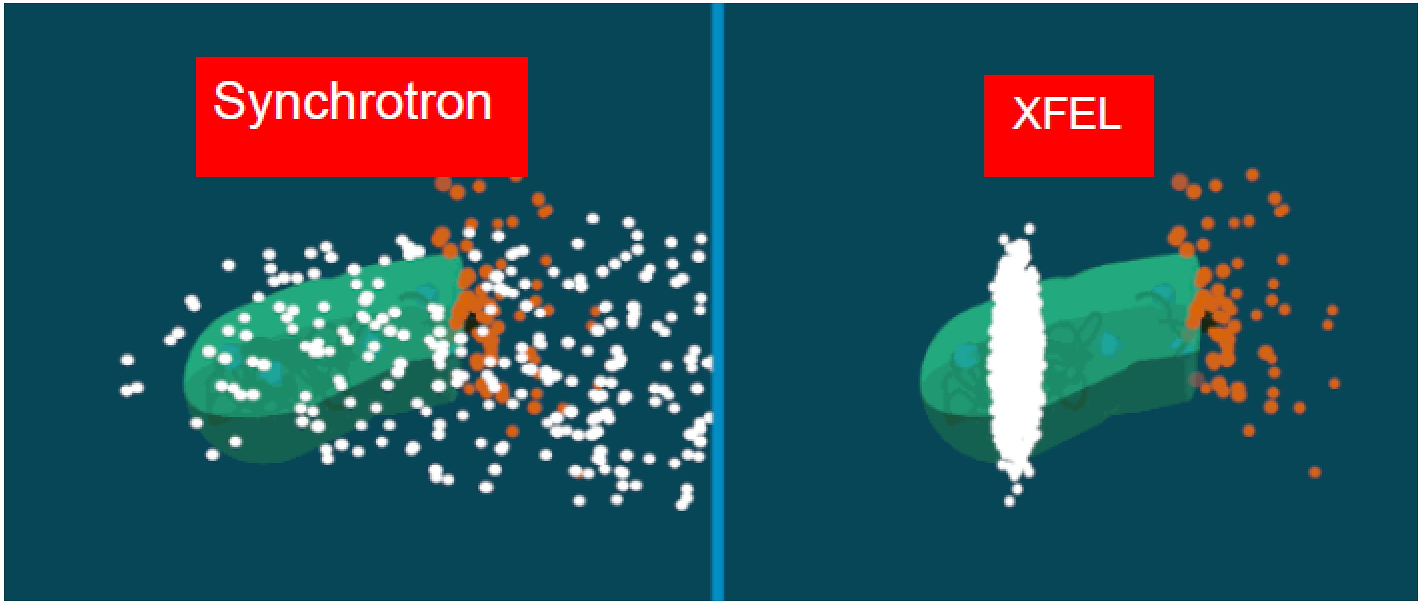

Credits: www.slac.stanford.edu

Beating radiation damage: Diffraction before Destruction

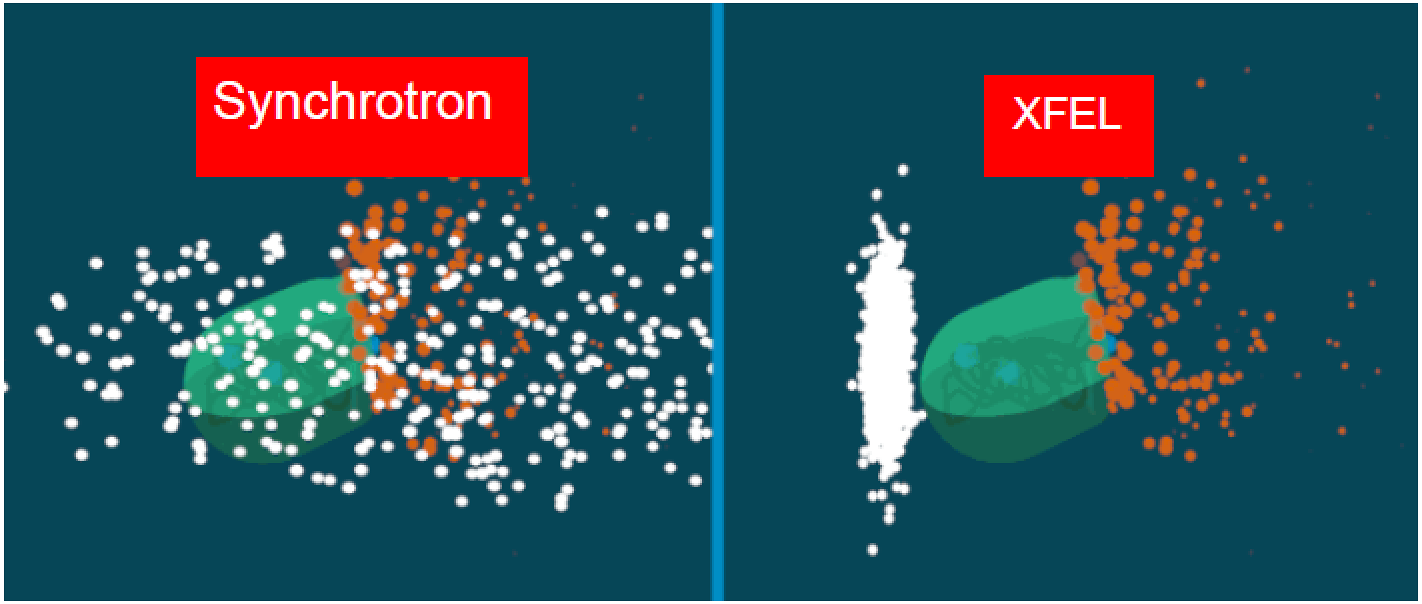

Credits: www.slac.stanford.edu

Diffraction before destruction

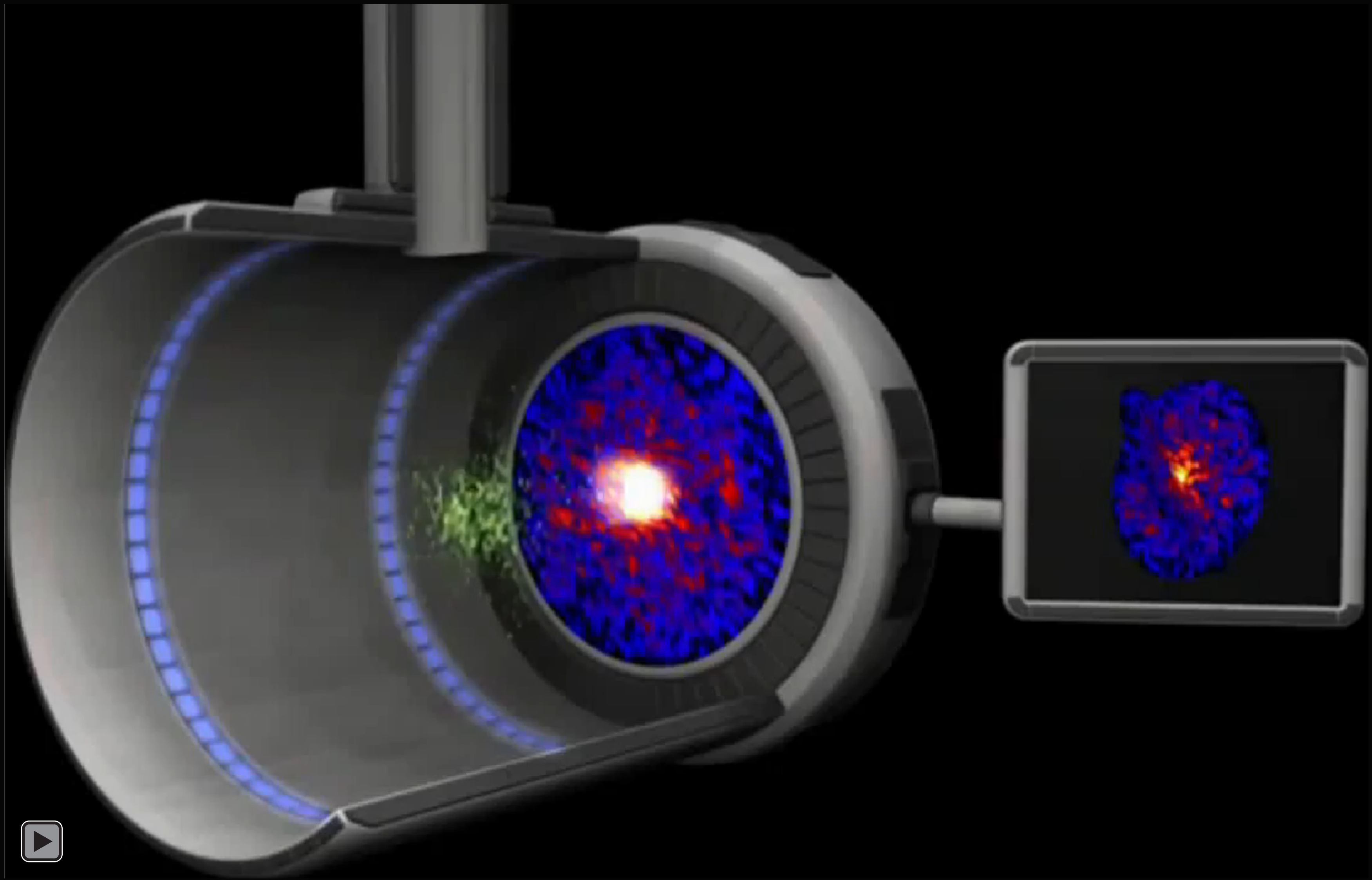

Possibilities of shooting at high frequencies and recording fast dynamic processes

A Seeded Amplier FEL

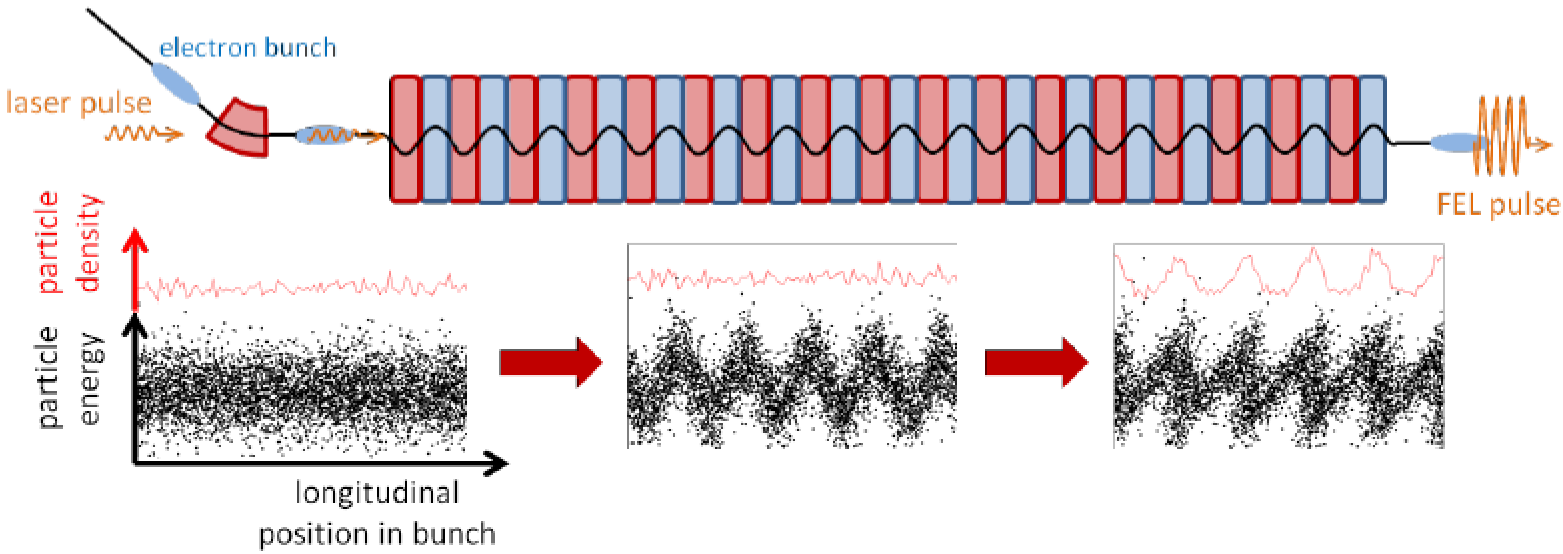

interaction with "seed" laser pulse leads to energy modulation

phase slip in undulator converts energy modulation to density modulation

particles within each microbunch radiate coherently

FERMI at Elettra (Italy)

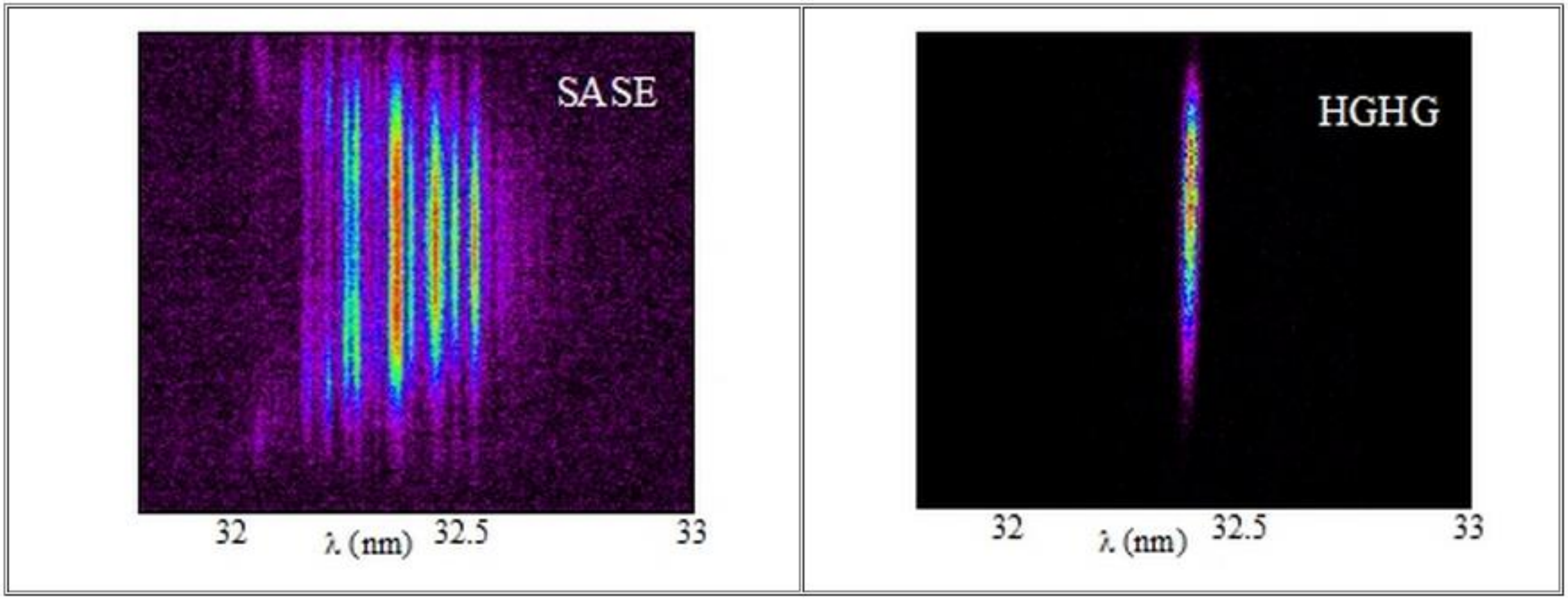

Figure 3. Single-shot FEL spectrum at 32 nm obtained in SASE (on the left) and in HGHG (on the right) mode at FERMI. While the horizontal axis is dispersed in wavelength, the vertical axis represents the vertical distribution of the FEL intensity at the spectrometer CCD. The energy per pulse provided in SASE mode by using the optical klystron technique is about 100 micro-joules and the bandwidth is 3.3×10^{-3}.

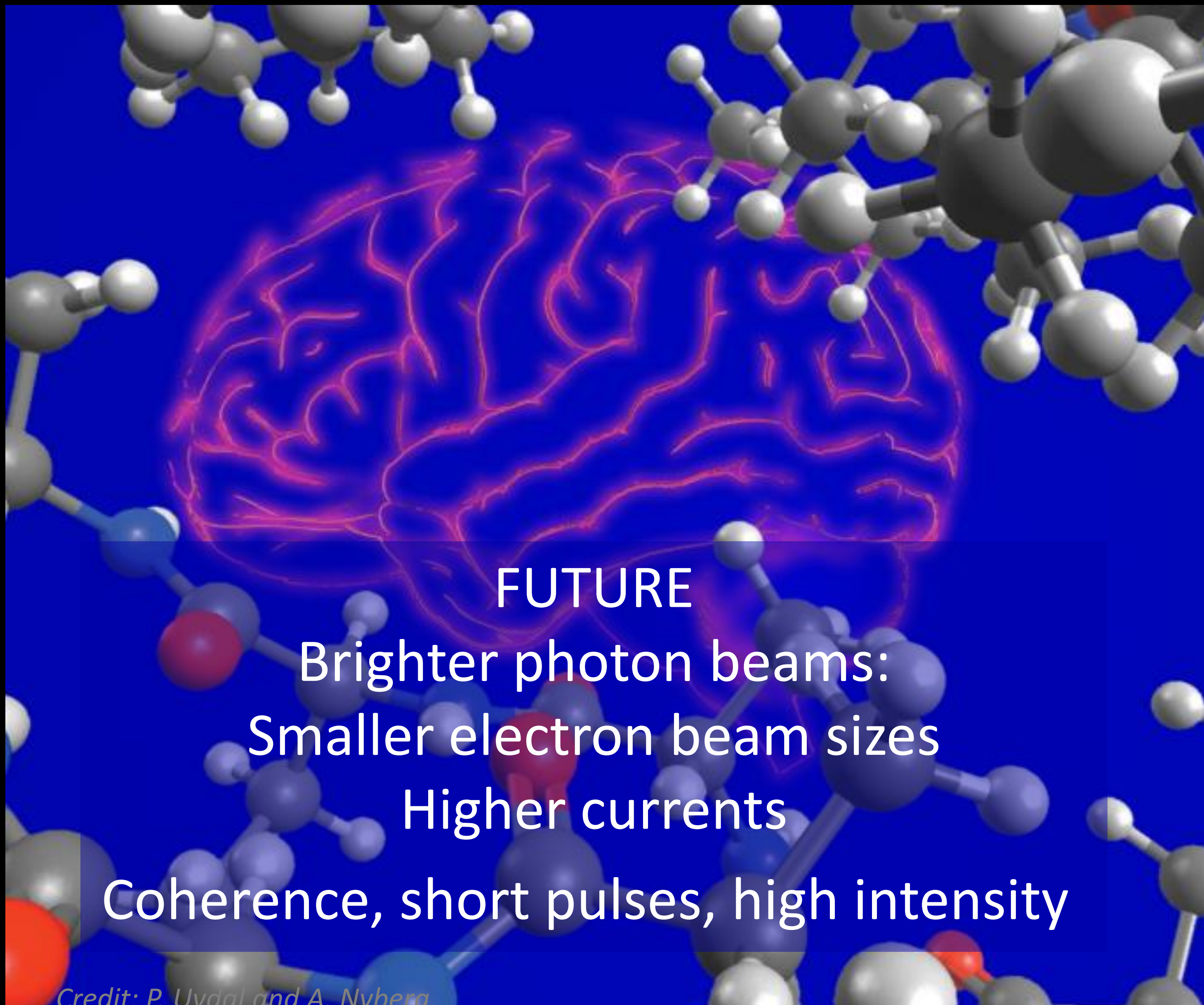

FUTURE

Brighter photon beams:

Smaller electron beam sizes

Higher currents

Coherence, short pulses, high intensity

Credit: P. Uvdal and A. Nyberg.

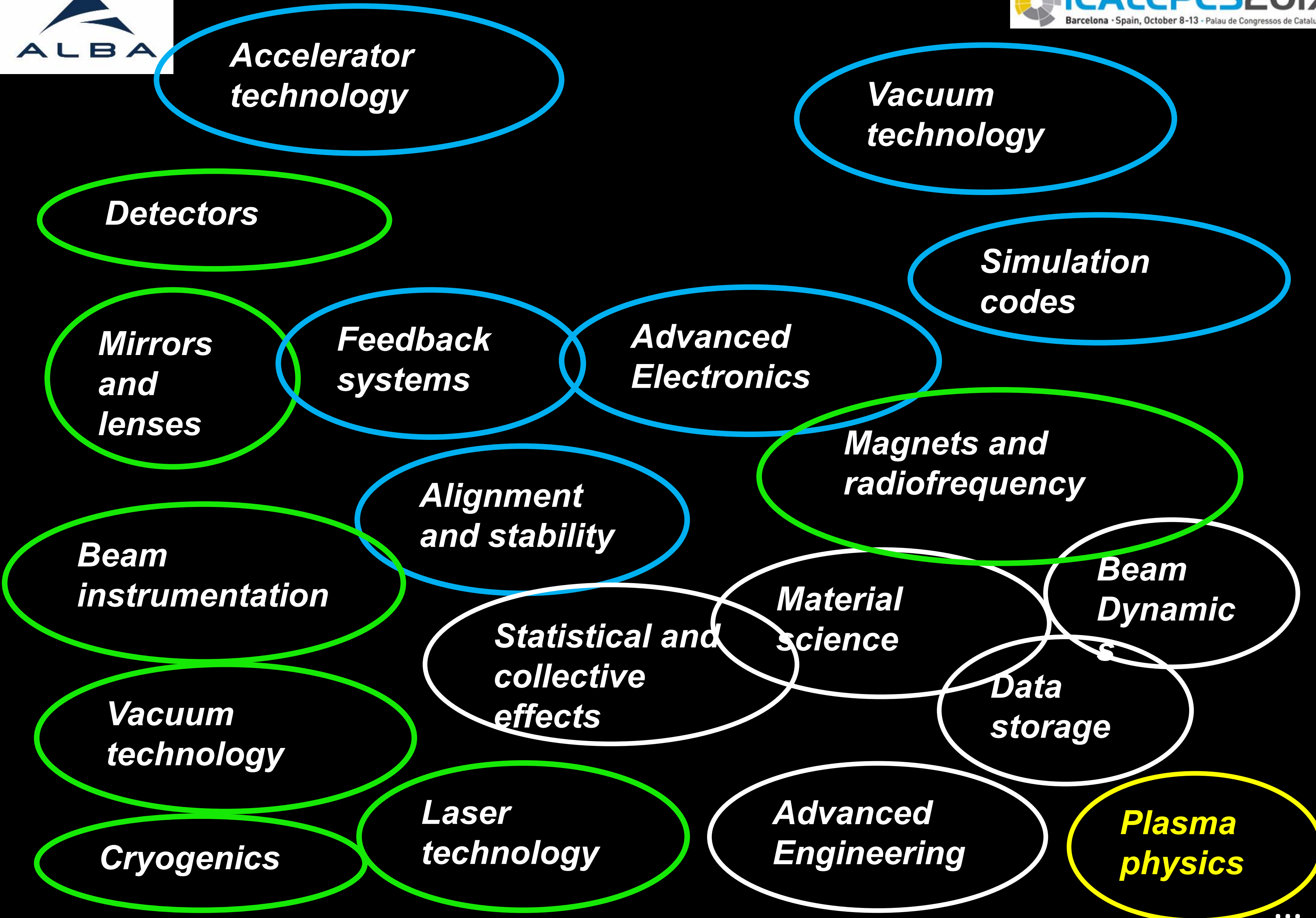

Accelerator technology
Vacuum technology
Detectors
Simulation codes
Mirrors and lenses
Feedback systems
Advanced Electronics
Magnets and radiofrequency
Alignment and stability
Beam instrumentation
Beam Dynamic s
Material science
Statistical and collective effects
Data storage
Vacuum technology
Laser technology
Advanced Engineering
Plasma physics
Cryogenics
…

Accelerator technology

Vacuum technology

CONTROLS & COMPUTERS

Detectors

Simulation codes

Mirrors and lenses

Feedback systems

Advanced Electronics

Magnets and radiofrequency

Alignment and stability

Beam instrumentation

Beam Dynamics

Material science

Statistical and collective effects

Data storage

Vacuum technology

Laser technology

Advanced Engineering

Cryogenics

Plasma physics

…

The frontier is moving ahead of us

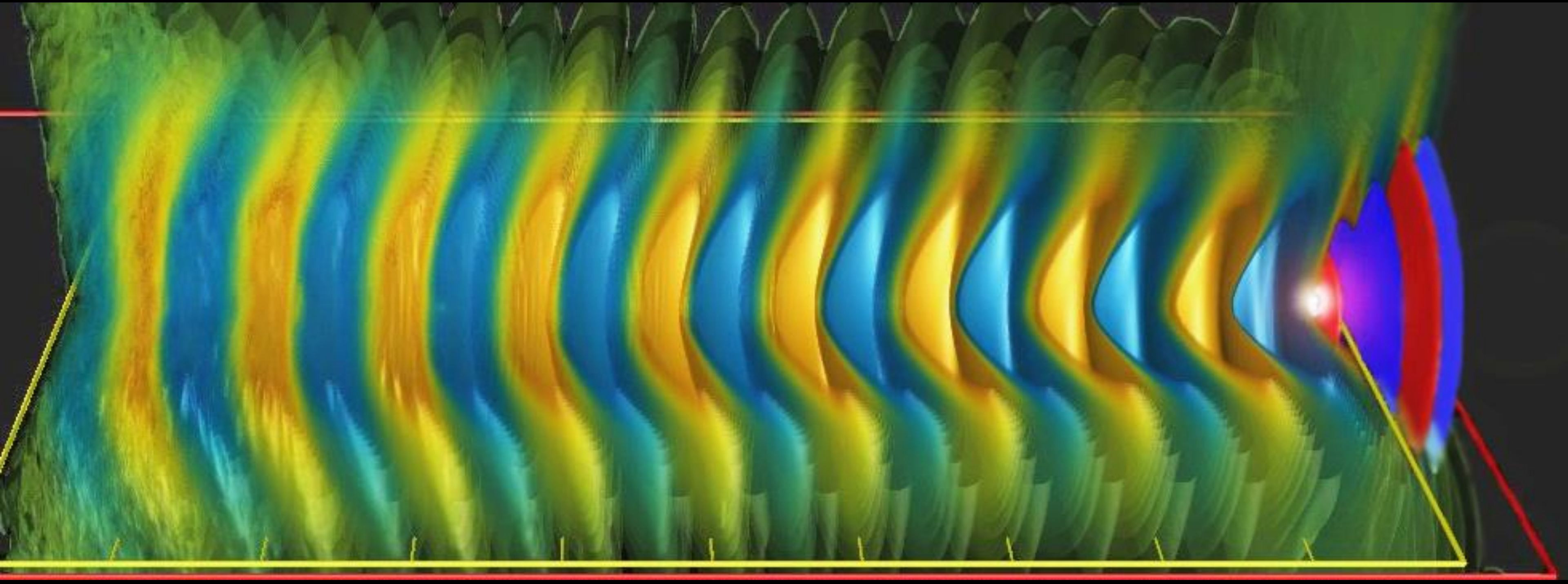

Simulation by Jean-Luc Vay and Cameron Geddes

Three examples of state of the art research with synchrotron and XFEL beams

1.- Transmission X ray microscope : cryo tomography and spectromicrsocopy

2.- 3D reconstruction with Ptychography

3.- Ultra fast chemical reaction viewed with fs time resolution

Salvador Ferrer, Alba light source

X ray microscopy. Basic concepts

Resolving power of a microscope proportional to λ . Visible light $\lambda \sim 500$ nm
X rays : $\lambda \sim$ 2nm - 0.1 nm

Visible light microscopes are based on the refraction of visible light by lenses

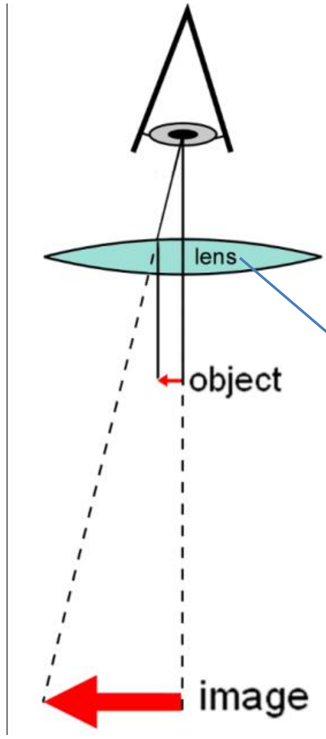

Refractive index n~ 1.5; $\sin\theta_i = n \sin\theta_f$ $\theta_i = 30^o$, $\theta_f = 19^o$

Which is the refractive index of X rays in materials?

n (Xray) = 0.9995 : very close to one

Fresnel Zone Plates : these are the lenses for X ray microscopy

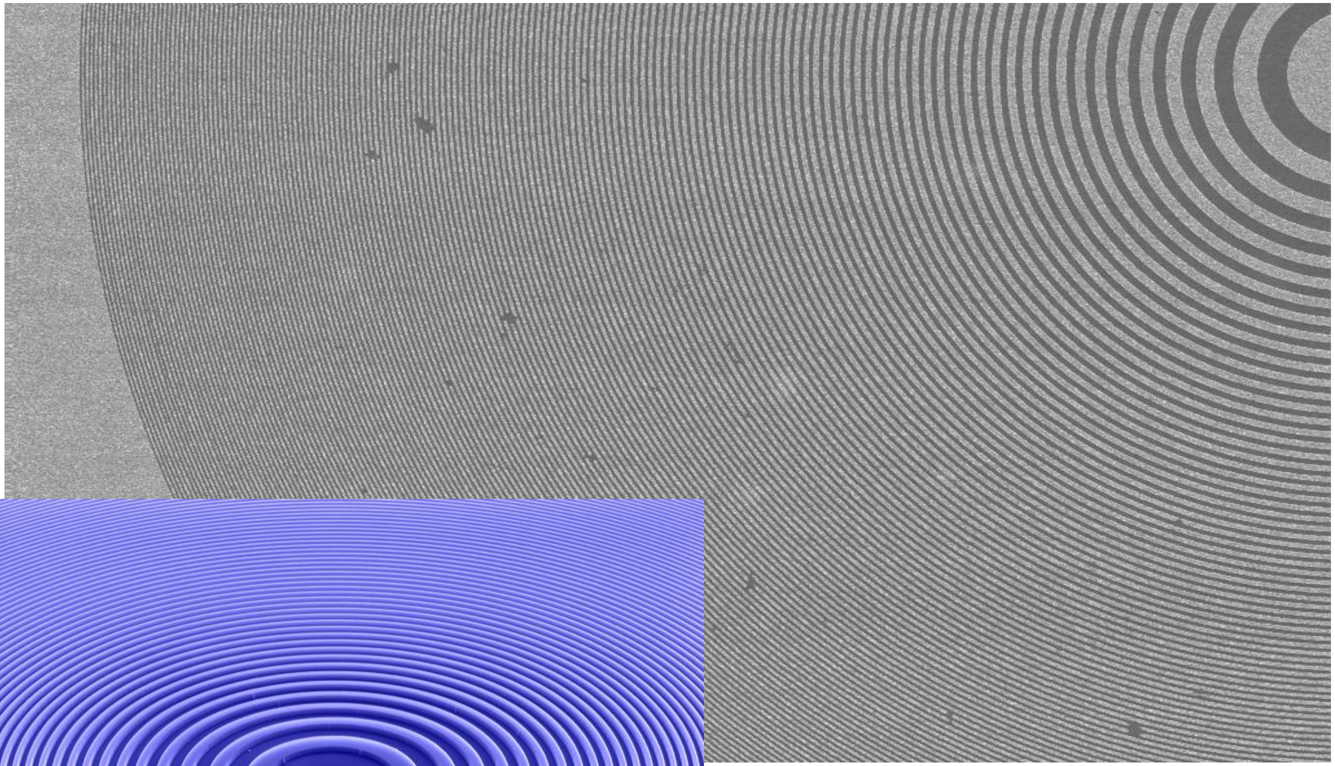

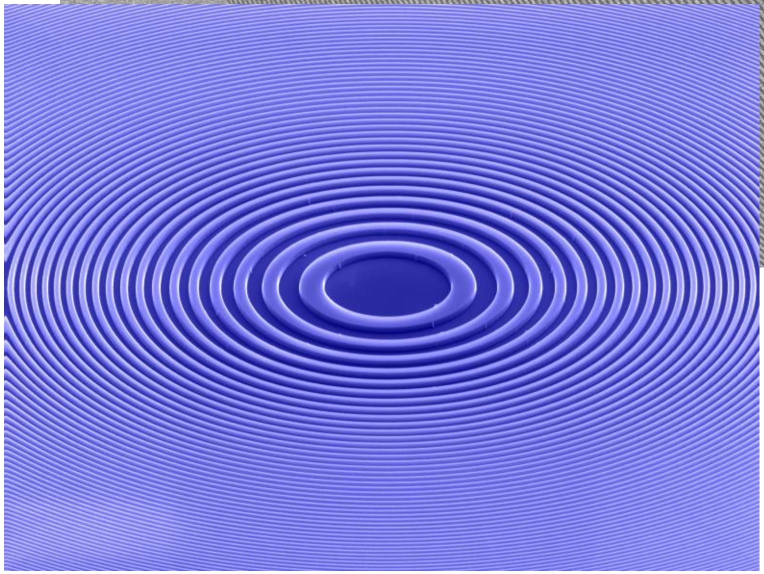

- Δr = 25 nm
- D = 63 μm
- N = 618 zones
- f = 650 μm
- NA = 0.05 @ λ = 2.4 nm

Alternate transparent and opaque zones.
Key optical components for X ray microscopy.

Mistral Microscope

JOURNAL OF SYNCHROTRON RADIATION

Andrea Sorrentino, Josep Nicolas, Ricardo Valcarcel, Francisco JavierChichon, Marc Rosanes, Jose Avila, Andrei Tkachuk, Jeff Irwin, Salvador Ferrer and Eva Pereiro

J. Synchrotron Rad. (2015). **22**, 1112–1117

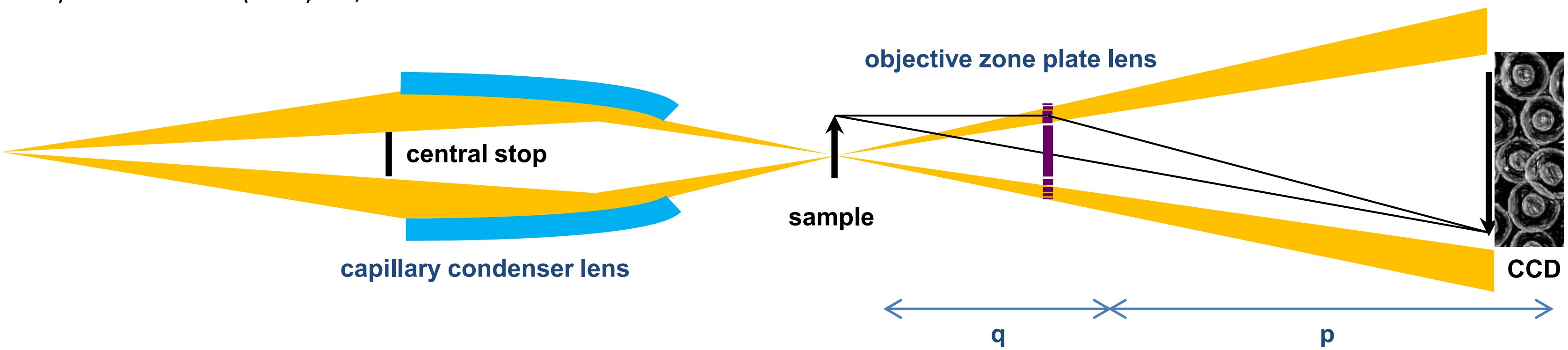

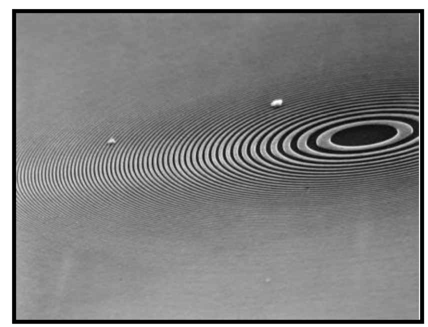

Soft X rays (λ = 2.5 nm, hν = 500 eV) go through the sample (10 μm thick) and produce absorption contrast.
Sample at low T to reduce X ray beam damage.
Tomography : Acquire images at different angle (-70º to 70 º steps of 0.1 º) : 3D reconstruction

Ultrastructural alterations of host cell during HCV infection

Ana Joaquina P. rez-Berná, Maria José Rodríguez, Francisco Javier Chichón,
Martina Friederike Friesland, Andrea Sorrentino, Jose L. Carrascosa, Eva Pereiro,
and Pablo Gastaminza

ACS NANO
DOI: 10.1021/acsnano.6b01374

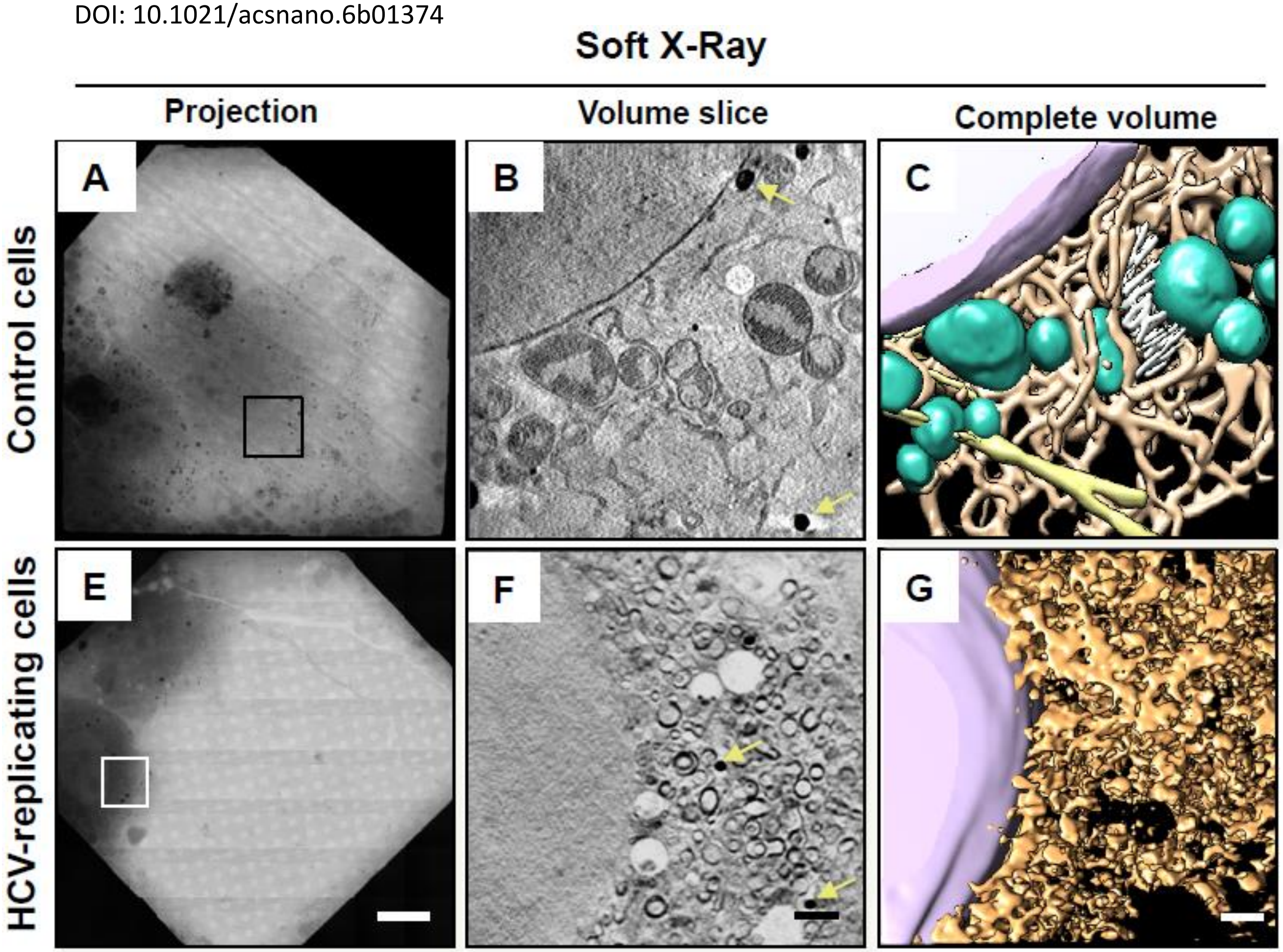

Nuclear Envelope | Mitochondria | Normal ER | Modified ER | Cytoskeleton | Golgi

Alteration of the mitochondria-ER contacts in HCV replicating cells

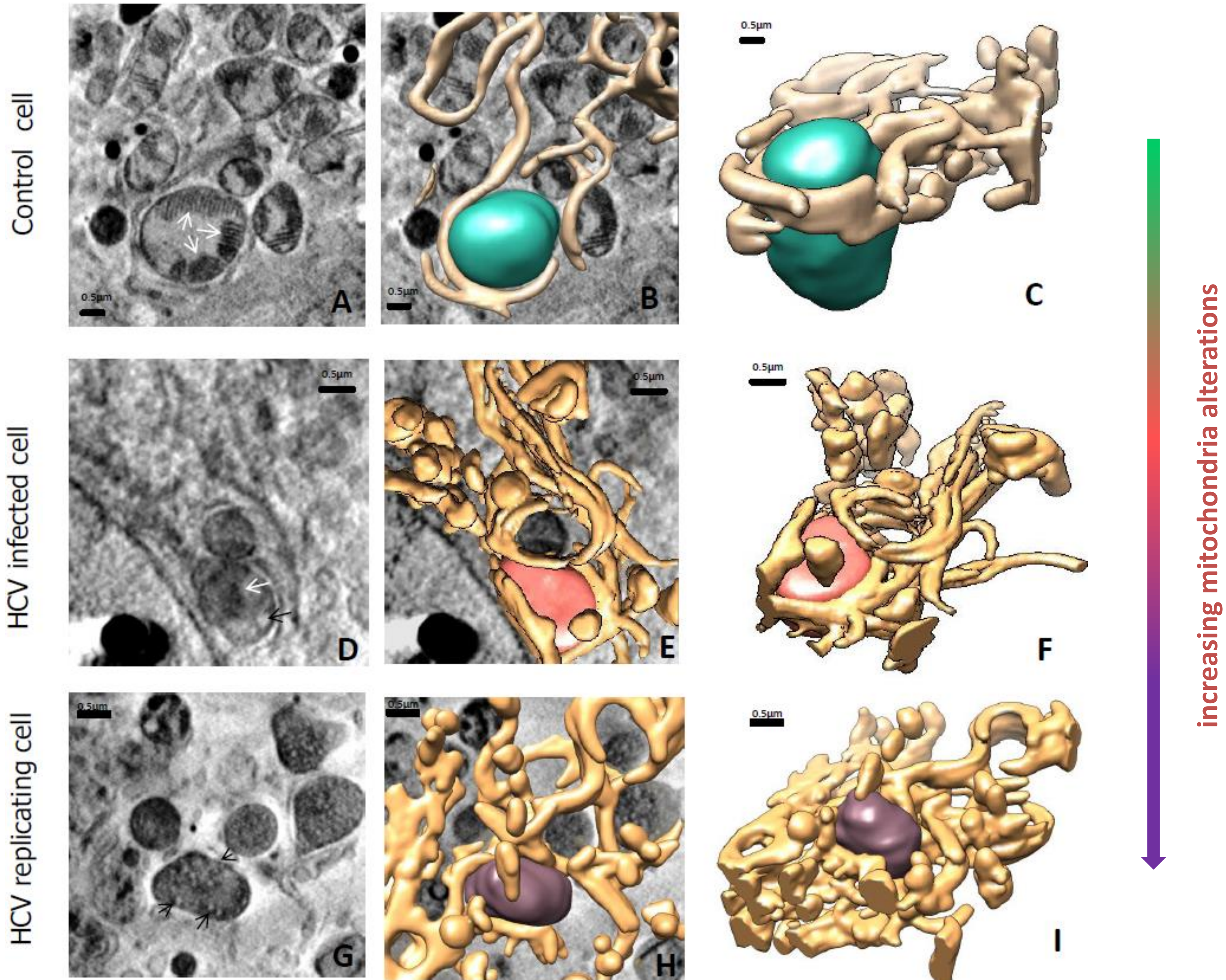

X ray absorption spectroscopy:

Absorption of X rays occurs at well defined energies characteristic of the absorbing atoms

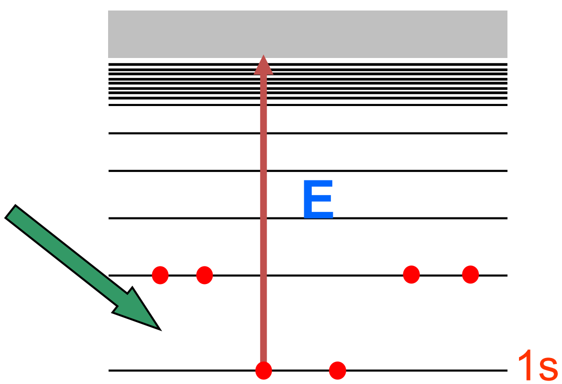

X rays
of variable energy

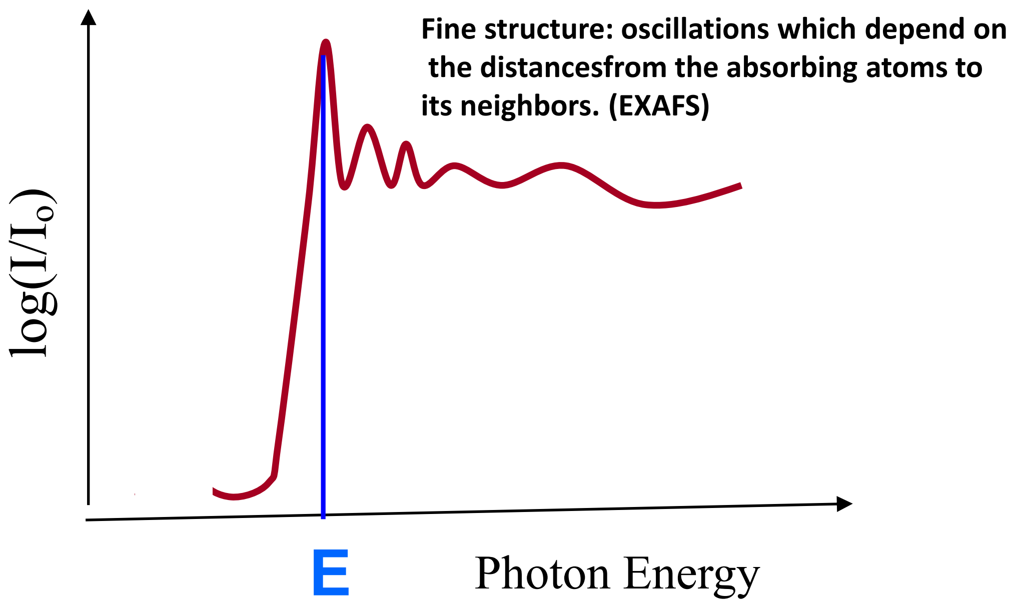

A vacuole-like compartment concentrates a disordered calcium phase in a key coccolithophorid alga

Sanja Sviben, Assaf Gal, Matthew A. Hood, Luca Bertinetti, Yael Politi, Mathieu Bennet, Praveen Krishnamoorthy, Andreas Schertel, Richard Wirth, Andrea Sorrentino, Eva Pereiro, Damien Faivre2 & Andre´ Scheffel1

DOI: 10.1038/ncomms11228

Coccoliths are calcitic particles produced inside the cells of unicellular marine algae known as coccolithophores. They are abundant components of sea-floor carbonates, and the stoichiometry of calcium to other elements in fossil coccoliths is widely used to infer past environmental conditions. Here we study cryo-preserved cells using state-of-the-art nanoscale imaging and spectroscopy. We identify a compartment, distinct from the coccolith-producing compartment, filled with high concentrations of a disordered form of calcium.

Our findings provide insights into calcium accumulation in this important calcifying organism.

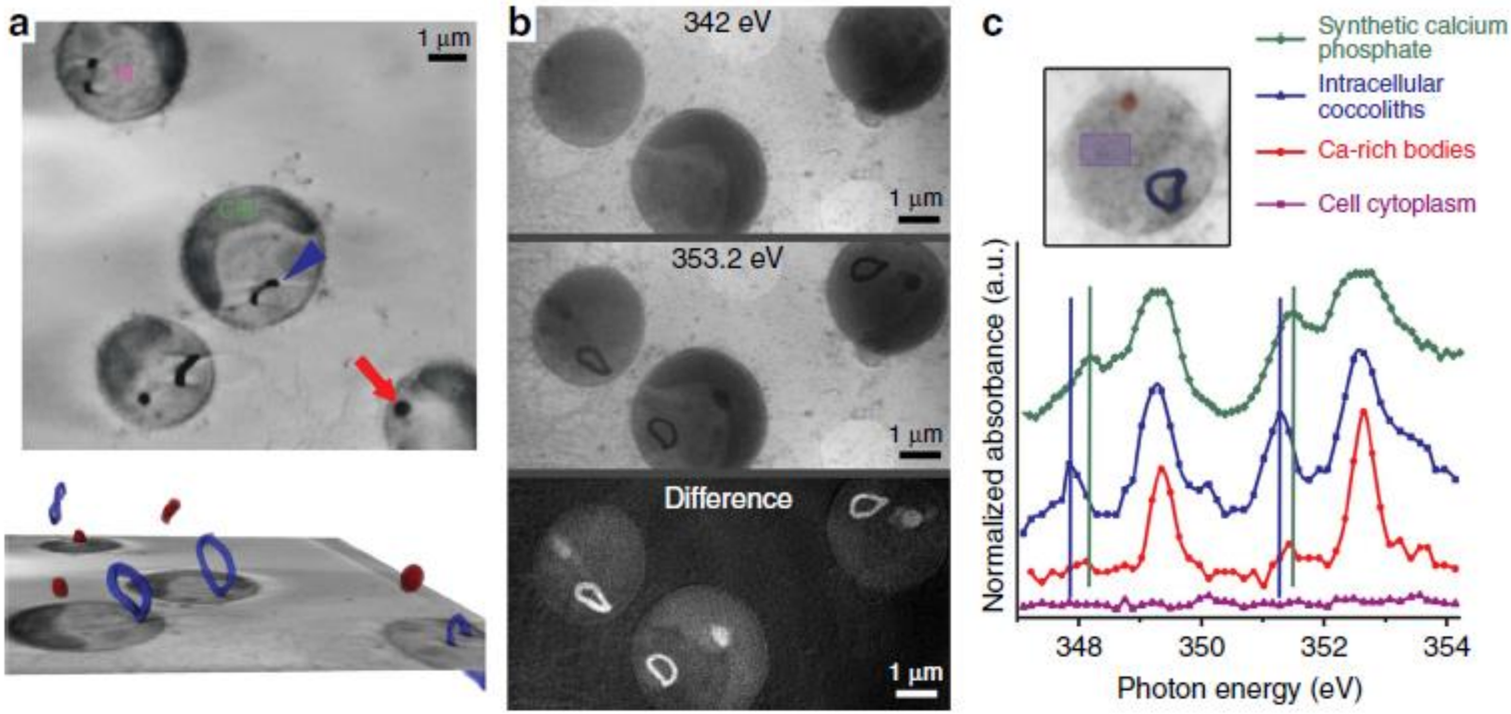

a: top 2D slices of a coccolith (arrow head) and a Ca rich body (red arrow)
bottom : 3D segmentation of the Ca rich body

b: X-ray images recorded at an energy below the Ca L2,3-egde (342 eV), at the edge energy (353.2 eV) and the grey value difference between both images

c: Averaged XANES spectra of the Ca L2,3-edge; the inset shows the exact locations in one of these cells nucleus chloroplast coccolith in statu nascendi

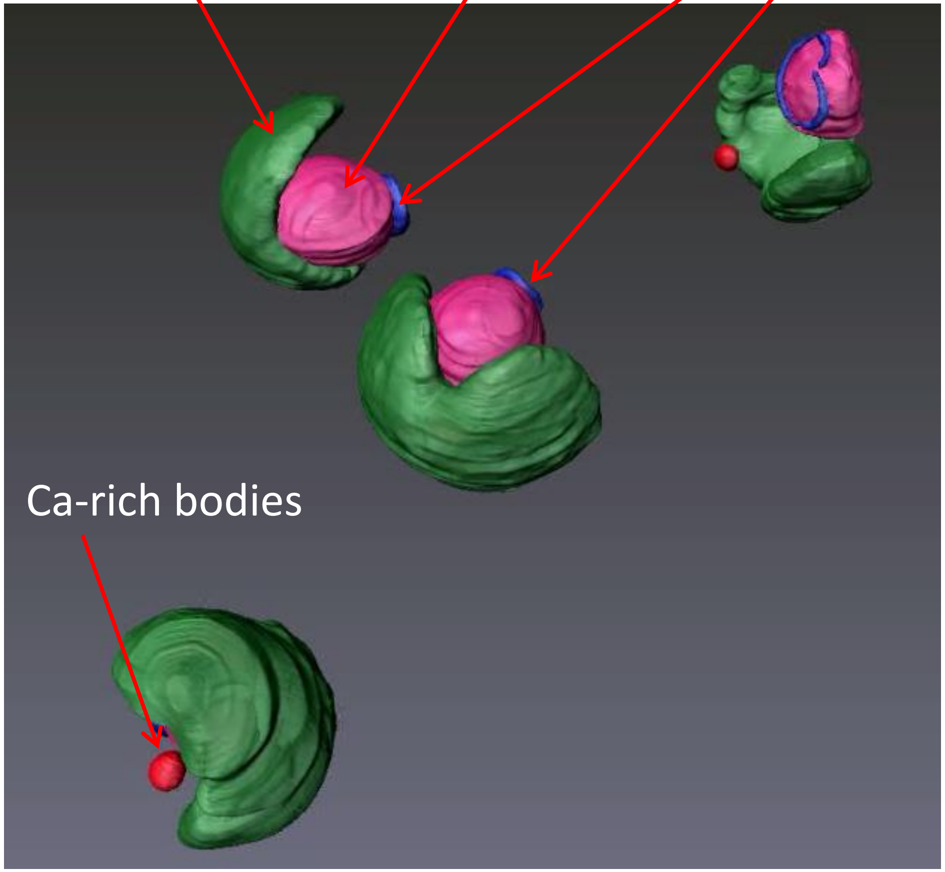

Advantages of the method:

1.- Few hundreds images is enough for 3D reconstruction. Acquisition time ~ 20-30 min.
2.- Simple reconstruction algorithms

Limitations : resolution 20-30 nm limited by Zone Plate manufacturing. Not easy to improve

Future perspectives: Phase contrast imaging to enhance contrast of similarly absorbing samples

High-resolution non-destructive three dimensional imaging of integrated circuits

Mirko Holler Mirko Holler, Manuel Guizar-Sicairos, Esther H. R. Tsai, Roberto Dinapoli, Elisabeth Müller, Oliver Bunk, Jörg Raabe & Gabriel Aeppli

doi:10.1038/nature21698 (March 2017)

It is impossible to image entire microelectronic ships non destructively since features are 3D and too small. This implies a lack of direct feedback between design and manufacturing processes and hampers quality control.

X ray ptychography , a high resolution coherent diffractive imaging technique can create 3D images of integrated circuits with resolution down to 15 nm. The experiments represent a major advance in chip inspection and reverse engineering over the traditional destructive electron microscopy and ion milling techniques

Coherent diffraction imaging : speckles due to interferences

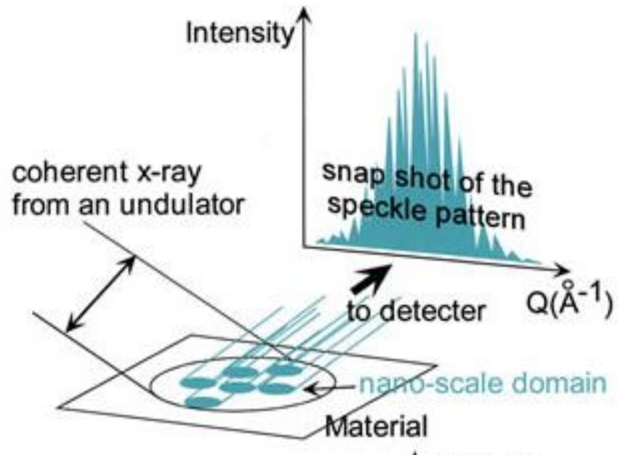

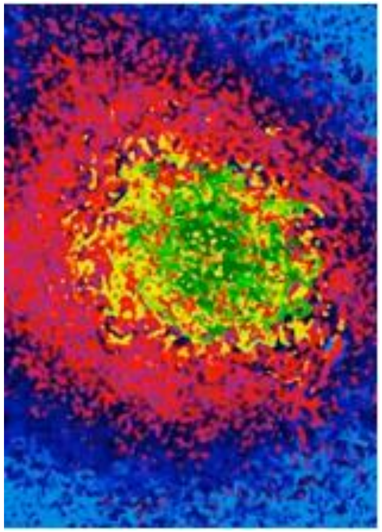

Ptychography : collect speckle patterns at different points of the sample with at least x2 oversampling

Ptychography at a collection of angles: tomographic Ptychography

Technique: ptychographic X-ray computed tomography (PXCT)

The speckle pattern originated from the diffraction of a coherent beam by the sample irregularities or density fluctuations is measured as a function of rotation and translation angle of the sample. The set of patterns is converted to a direct space 3D image with a resolution determined by the noise level of the patterns

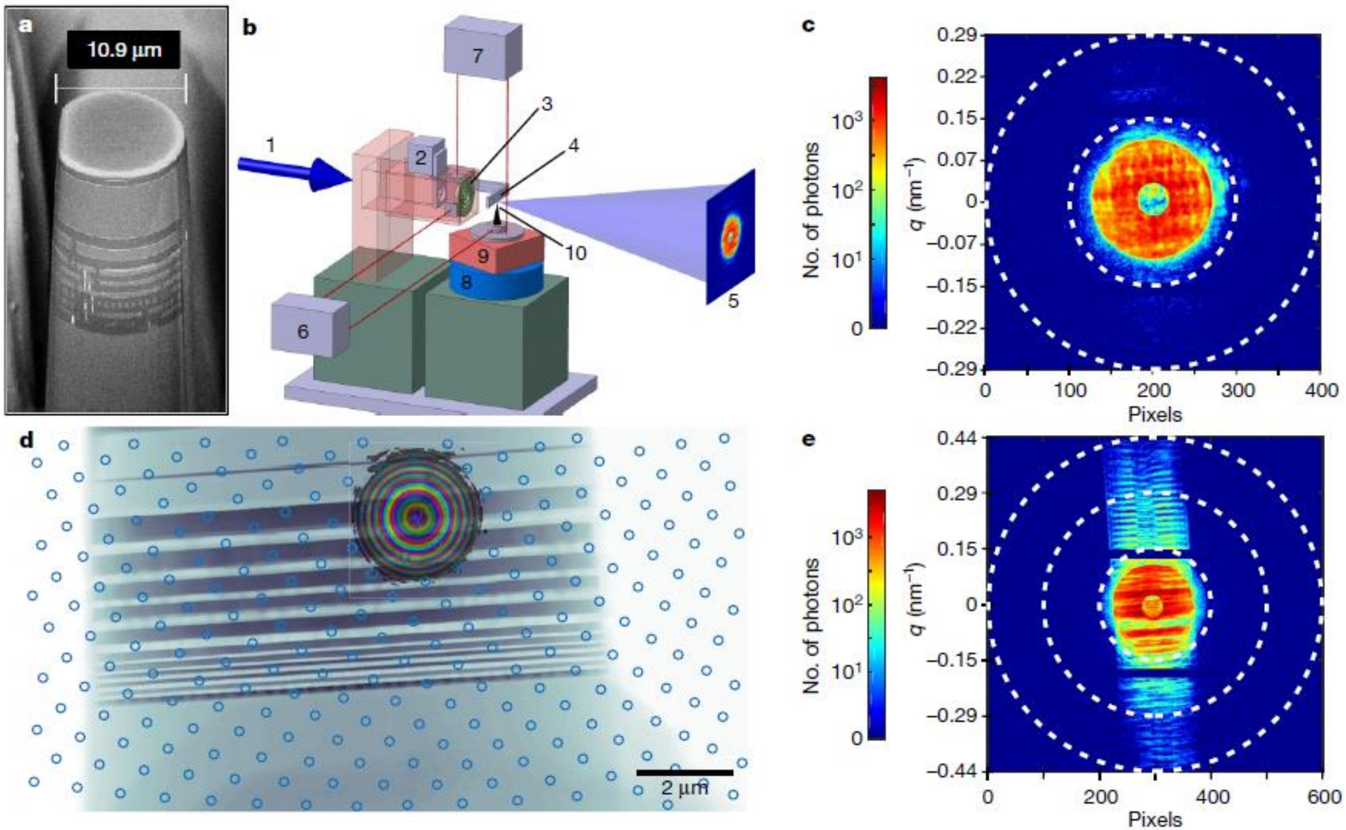

a: cylindrical sample

b: 1: 6 keV beam
3: Fresnel ZP
6,7 interferometers
9: piezo scanner
10: sample

c:diffraction pattern from a ASIC chip (1/235000)

d:recosntructed 2D projection and scanning positions

e: diffraction pattern from a ASIC chip

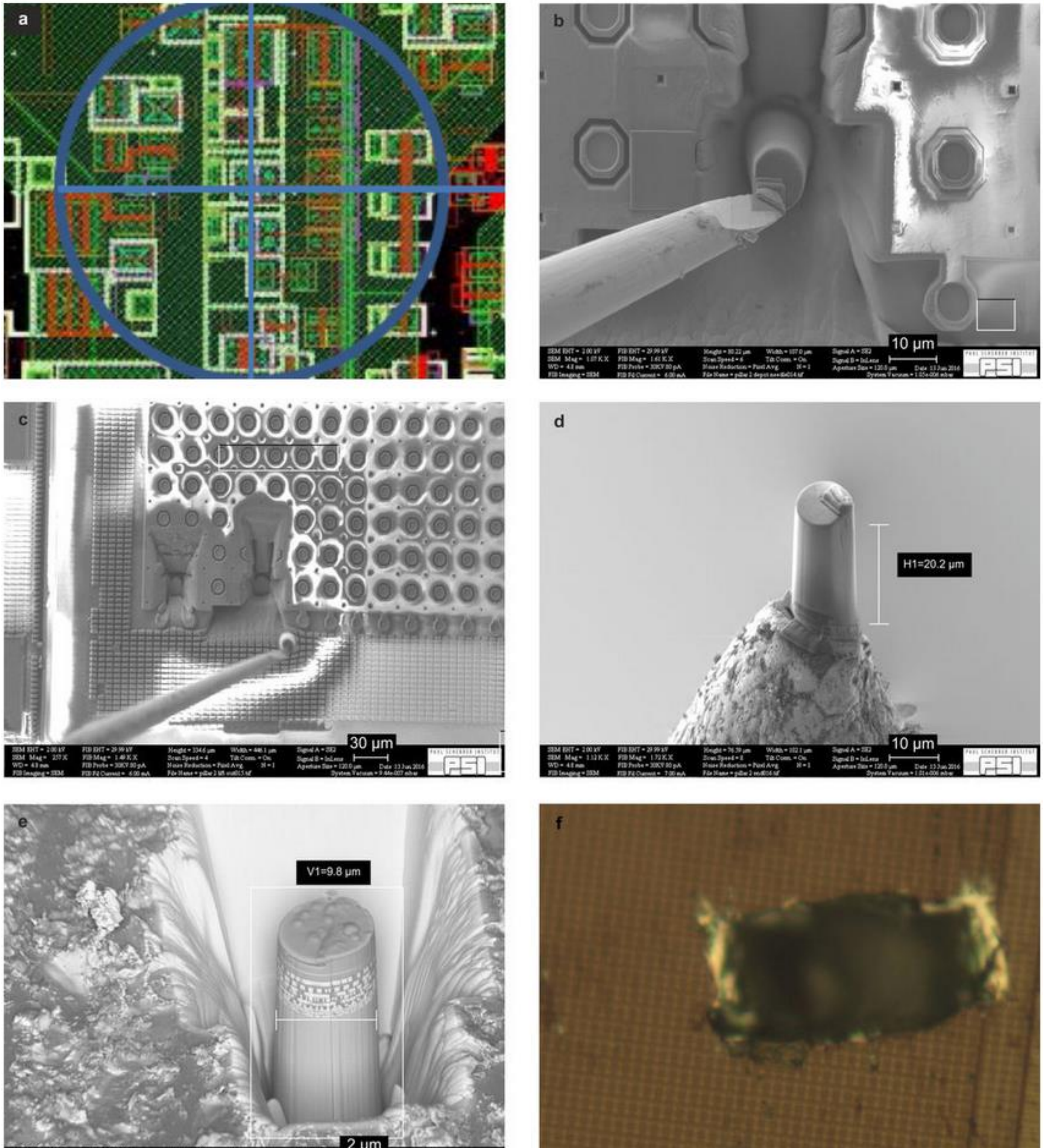
a
b
10 µm
c
30 µm
d
H1=20.2 µm
10 µm
e
V1=9.8 µm
2 µm
f

Results: ASIC chip (of PSI pixel detector)

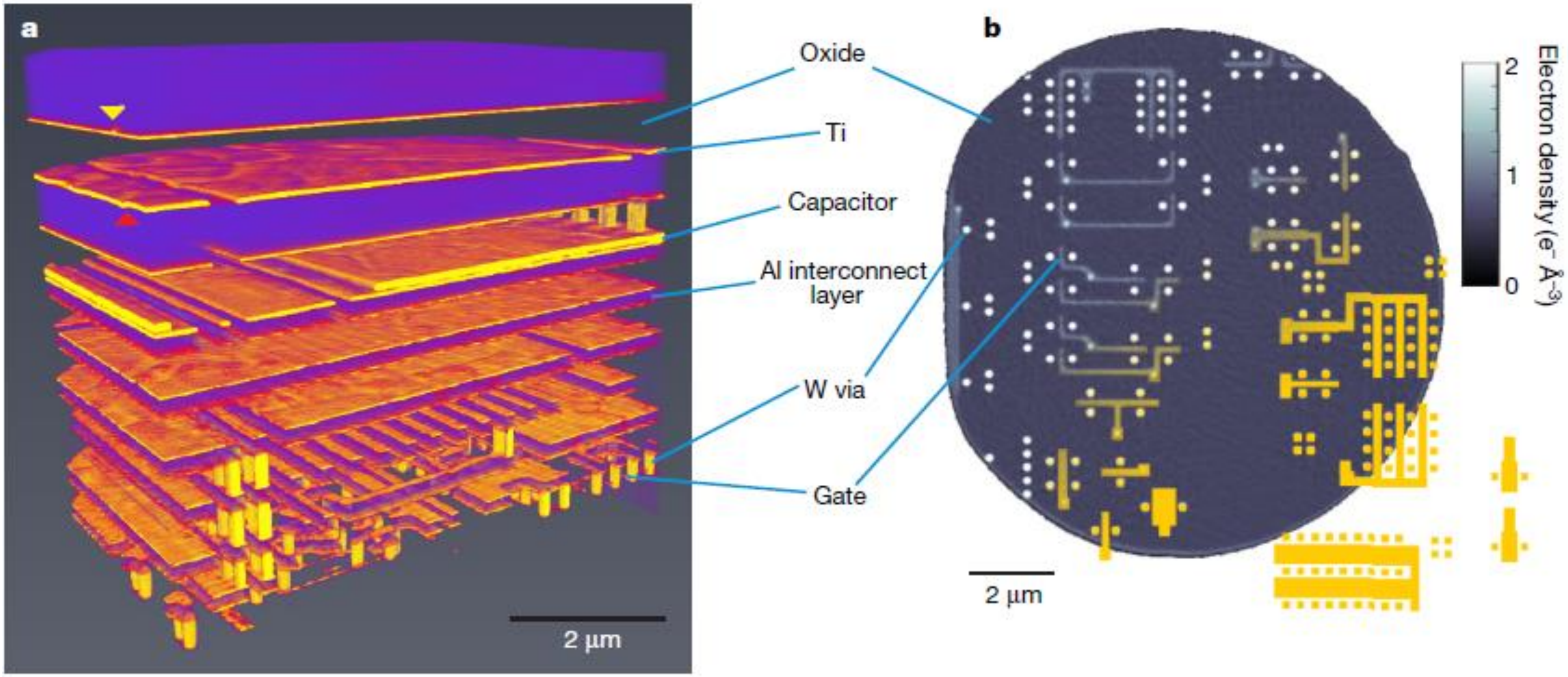

Fraction of the chip selected: set-reset memory latch

a) ▼ : manufacturing fault in Ti layer

▲ : waviness of the AlTi layer

b) Axial section across the second lowest layer, which contains the transistor gates; the grey scale (top right) represents electron density (in e− Å−3). The corresponding layer from the design file is shown as the partial overlay in yellow

22 nm technology Intel processor

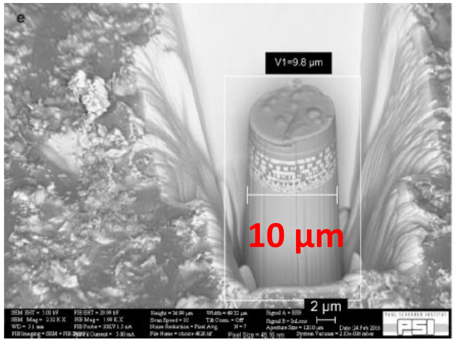

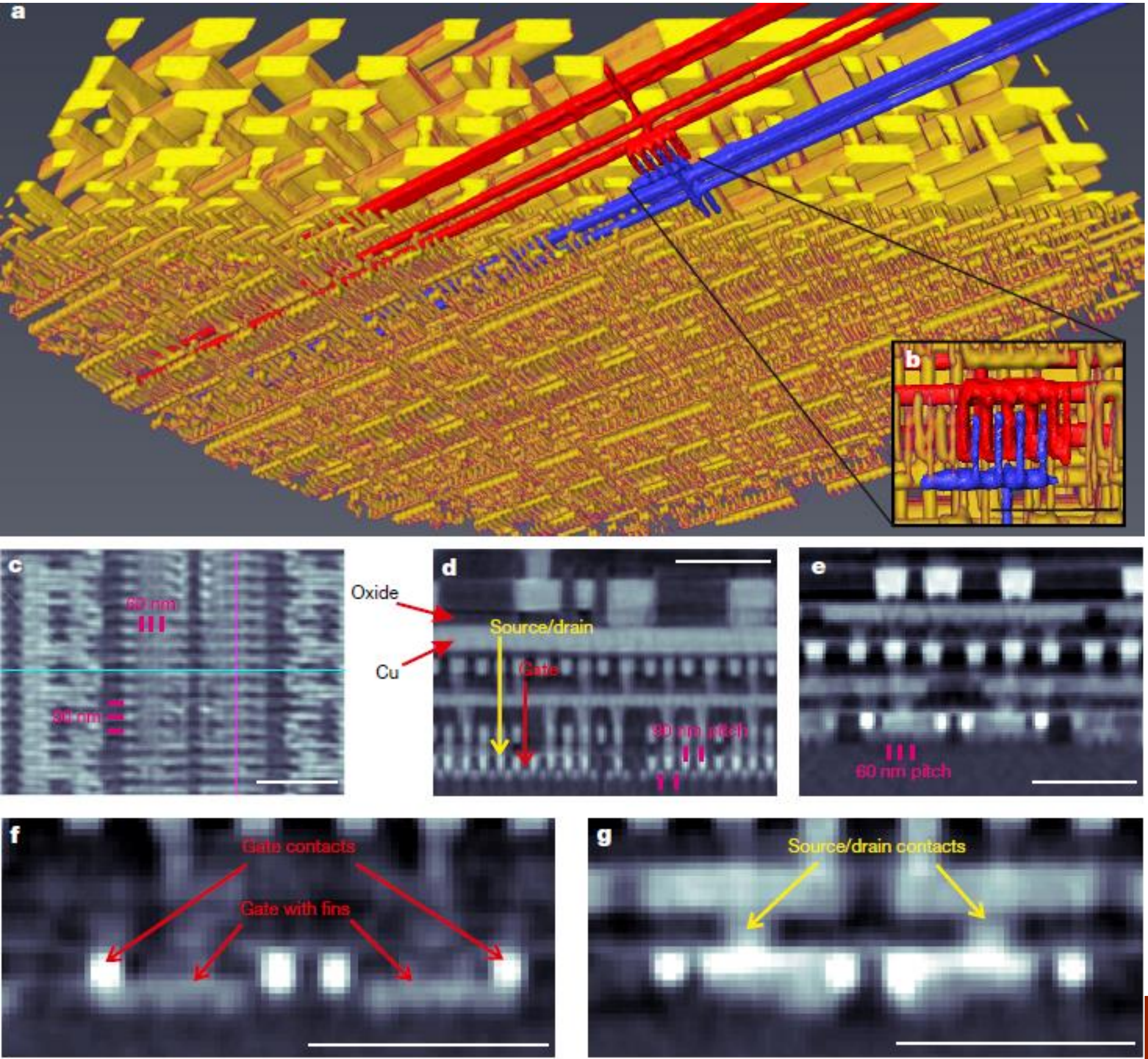

c: axial slice : parallel to the plane of the chip

d: coronal slice orthogonal to c along line in c. Pich of contacts 90 nm

e: sagittal slice orthogonal to c and d

f: sagittal slice along red arrow in d (plane of the gates)

Scale: 500 nm

Technical details :

Incoming beam 20 μm (H slit), hν = 6 keV , E/ΔE= 10^4, field of view 16x12 μm^2. Beam at sample position: 4 μm

Present limitations

1.- Cylindrical samples for having constant transmission
2.- Thin (~ 10 μm) samples
3.- long time required (Intel chip: 66 s/projection x 1200 projections = 22 hours ; 235000 images)

Future perspectives

1.- flat samples. Use laminography. Extended (mm^2) scanning areas
2.- Increase photon energy
3.- increase of coherent flux in 4^{th} generation facilities: ε_X : x 1/10 → x100 Coherent Flux
4.- better adapted optics : E/ΔE= 10^3 and more efficient focusing : → ~ x100
5.- Faster detectors and continuous sample scans

Possibility of practical usage of this non destructive method for inspection of integrated circuits with 10 nm resolution.

BIOCHEMISTRY

Mara et al., Science 356, 1276–1280 (2017) 23 June 2017

Metalloprotein entatic control of ligand-metal bonds quantified by ultrafast x-ray spectroscopy

Michael W. Mara, ... Edward I. Solomon[1]

The protein cytochrome c (cyt c) plays a key role in e- transport and adoptosis switching function by modulating a Fe-S bond . This bond was investigated by provoking its rupture with a laser pulse and reformation with XFEL pulses. The bond strength was determined and understood.

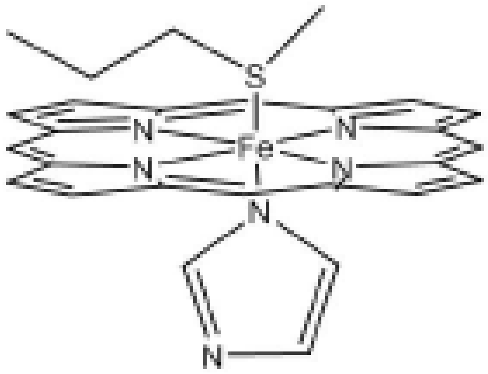

Fe oscillates between III and II oxidation states
The loss of FeIII-S bond plays a role in aptosis.

XAS : Si111 monochromator (1eV res.)

XES: spectrometer

Liquid jet diam. 100 µm

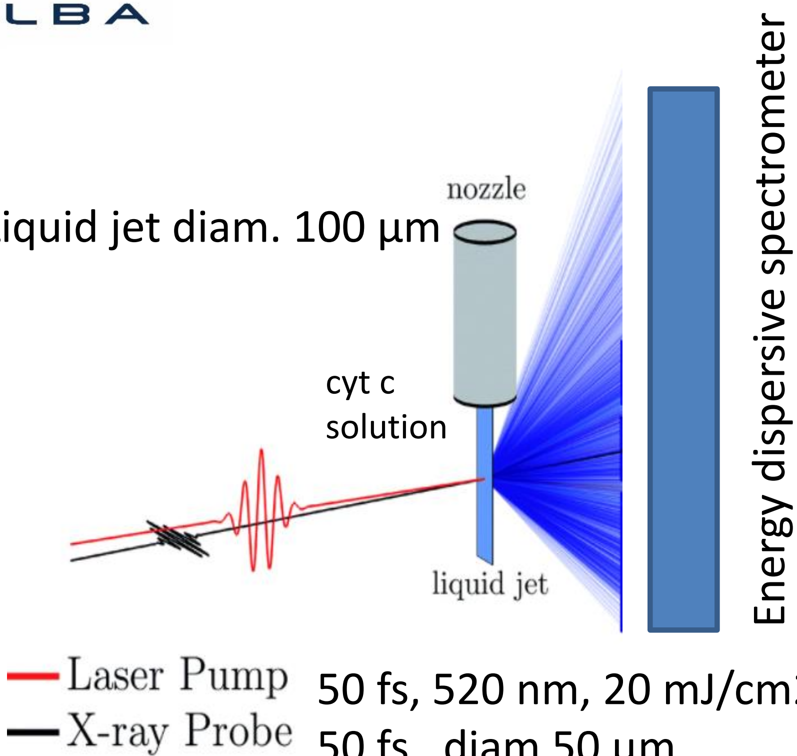

50 fs, 520 nm, 20 mJ/cm2

50 fs , diam 50 µm

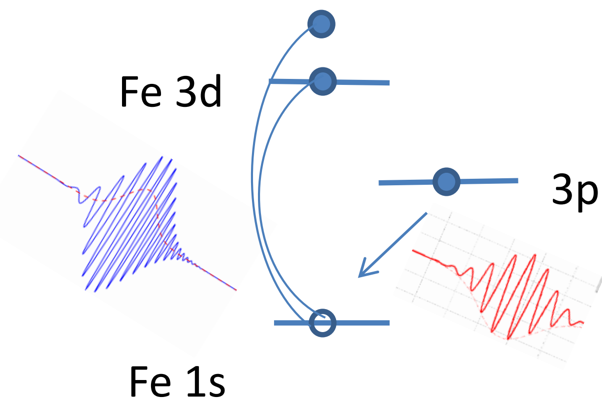

absorption emission

Laser fluence optimized for maximum population of excited states

Absorption allows to determine the atomic environment of the Fe since Energy shifts of the spectra indicate change in oxidation state

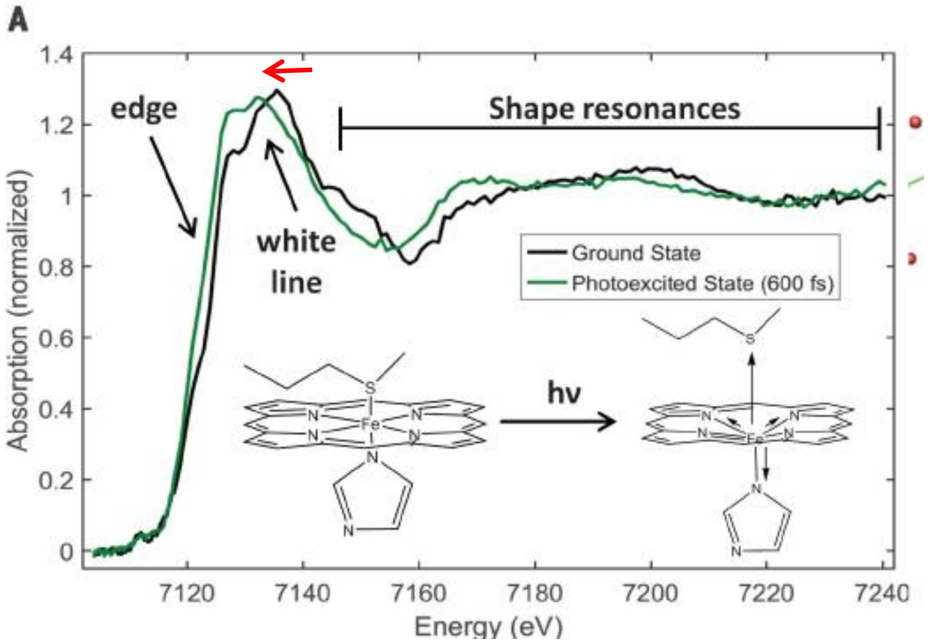

The energy shift ← is due to change between 6 coordination to 5 coor.

The excited state has FeII-N bonds elongated and the loss of Fe-S bond

Ground-State Fit Parameters:	Photoexcited-State Fit Parameters:
$\chi 2 = 2.4$	$\chi 2 = 1.9$
Fe-N(His): 1.95 Å	Fe-N(His): 2.15 Å
Fe-N(Por): 2.00 Å	Fe-N(Por): 2.09 Å
Fe-S(Met): 2.29 Å	Fe-S(Met): 3.04 Å

Emission spectroscopy senses the spin state (number of unpaired 3d e-)

Quintet (S_{Fe}=2)

Singlet (S_{Fe}=0)

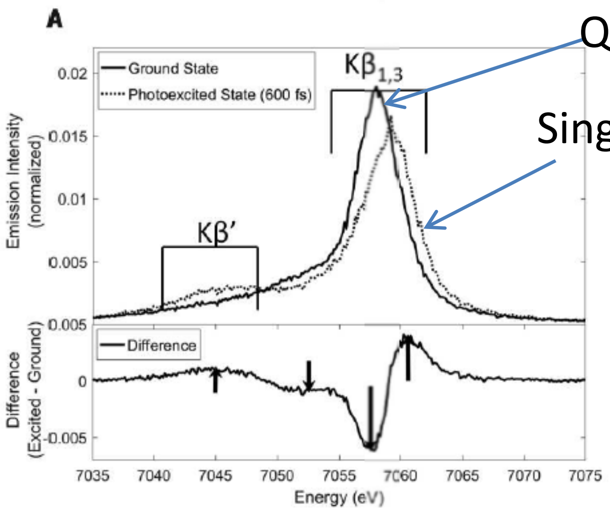

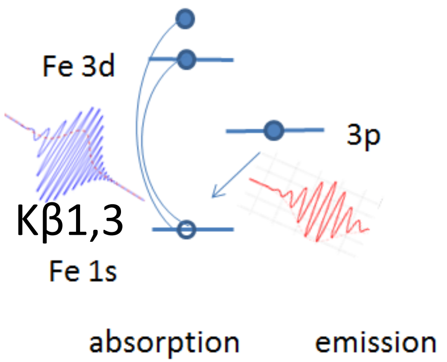

The loss of the Fe-S bond is associated to a change from 0 to 4 unpaired e-

Low Spin, S = 0	High Spin, S = 2
$(d_{xy})^2(d_{xz,yz})^4(d_{z2})^0(d_{x2-y2})^0$	$(d_{xy})^2(d_{xz,yz})^2(d_{z2})^1(d_{x2-y2})^1$

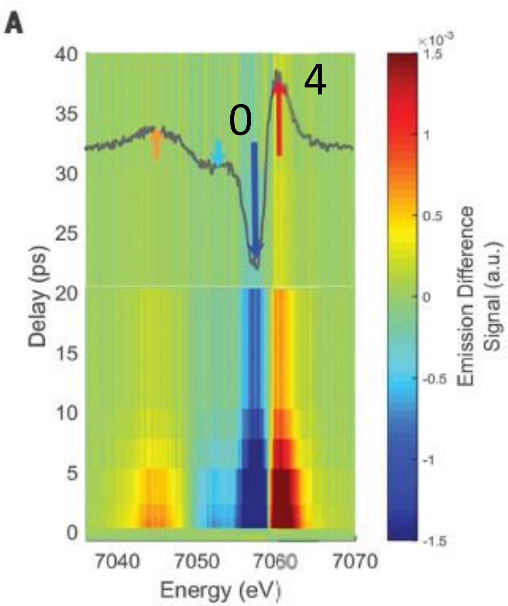

The evolution of the spins state for different delays allows to determine their characteristics times

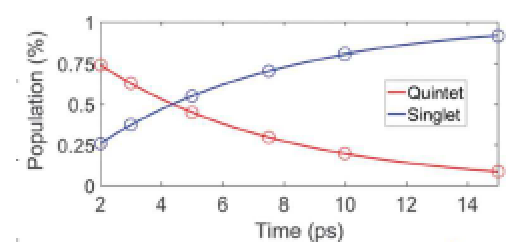

And its thermodynamics:

ΔH = 6.5 ± 1.2 kcal/mol
ΔS = 16 ± 3.2 cal/(mol*K)

Limitation:

By nature the pulses of the spontaneous emission FELS are chaotic (shot noise ampl.):

Longitudinal coherence properties

Temporal (top) and spectral (bottom) distributions of a single radiation pulse

I/I0 normalization of XAS signals is not simple

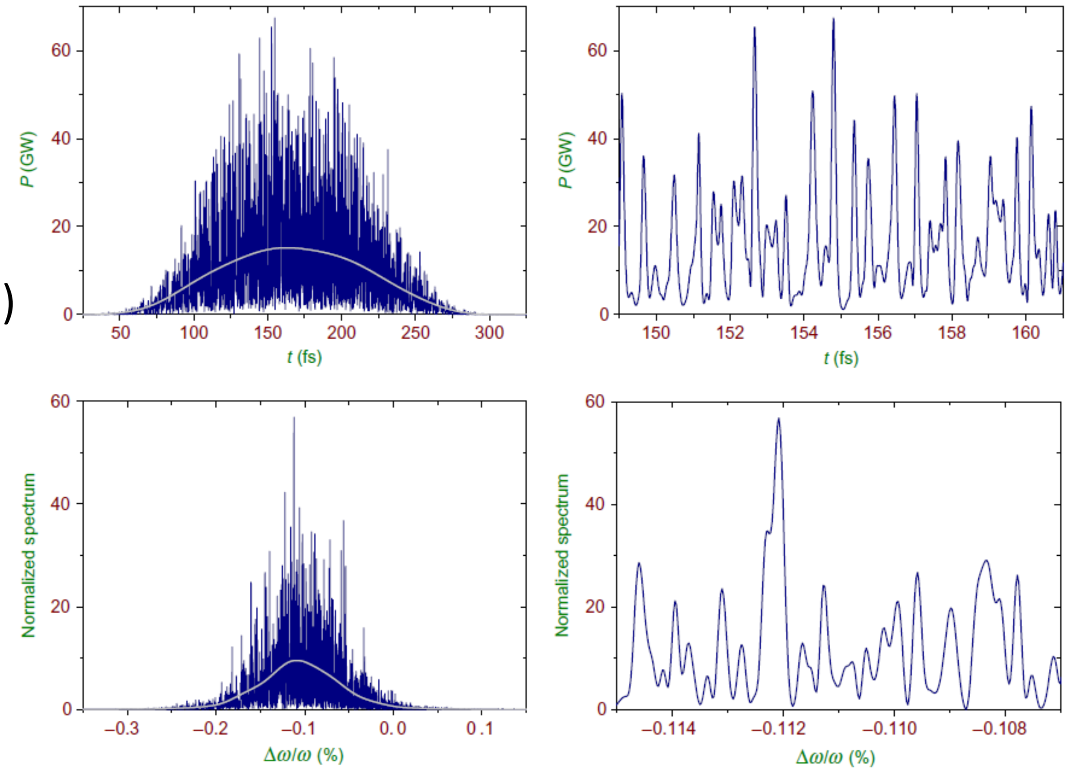

EXFEL, SASE1 at λ = 1 Å

(G. Geloni et al. *New Journal of Physics* **12** (2010) 035021)

Advantage: extremely high number of photons per pulse 10^{12} - 10^{13} photons /s

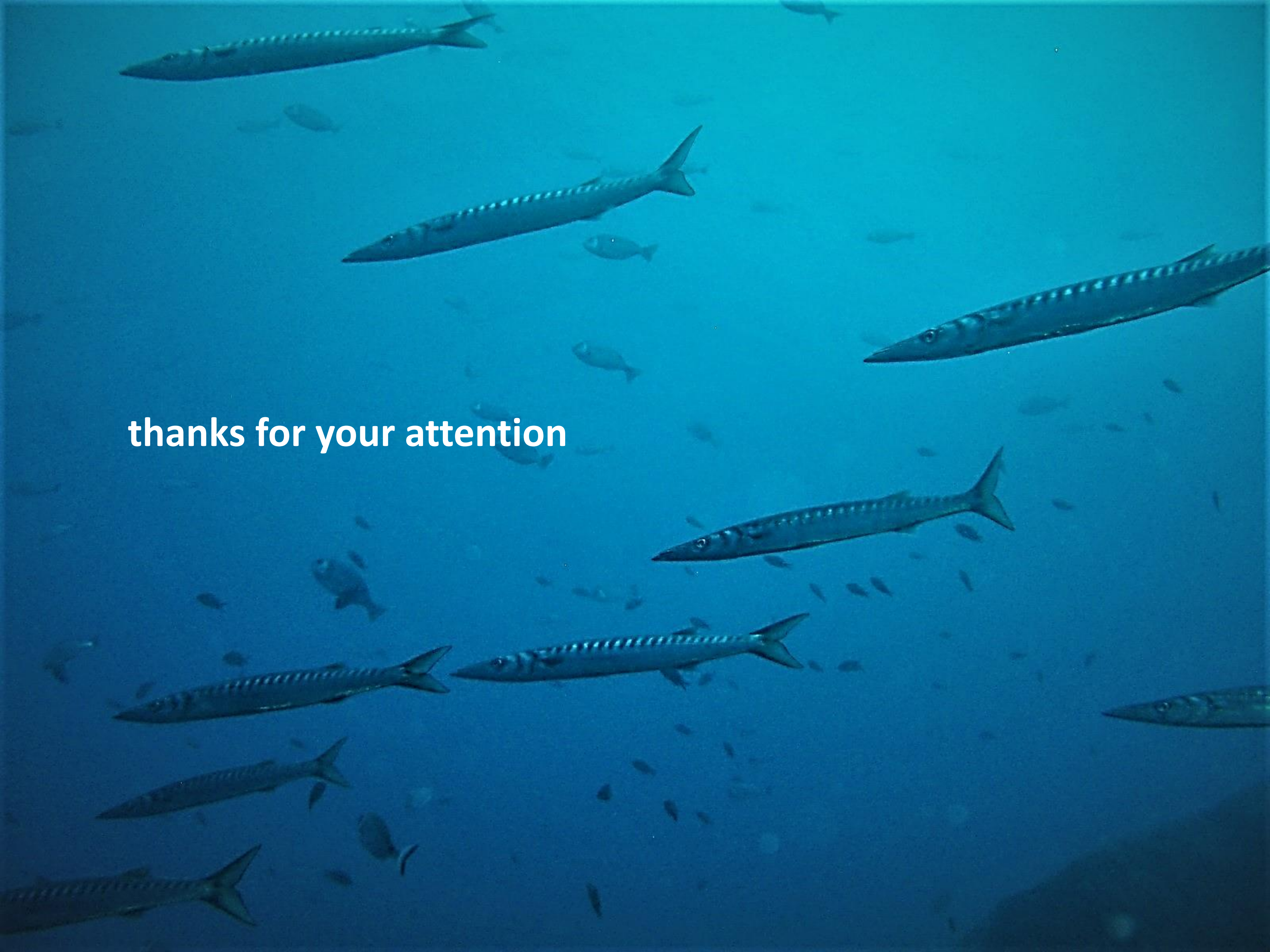
thanks for your attention